University of Alberta

Laboratory Study of High Temperature Corrosion in Petroleum Refineries

by

Nana Li 

A thesis submitted to the Faculty of Graduate Studies and Research in partial fulfillment of the requirements for the degree of

Master of Science

In

Materials Engineering

Department of Chemical and Materials Engineering

Edmonton, Alberta

Spring 2009

Your file Votre référence
ISBN: 978-0-494-54960-5
Our file Notre référence
ISBN: 978-0-494-54960-5

ABSTRACT

High temperature corrosion, caused by organic acids and sulfur compounds, continues to cause reliability issues in petroleum refineries. However, neither total sulfur contents measured by elemental analyses nor total acid contents measured by total acid number (TAN) have been found to correlate well with corrosivity.

A fundamental study of the relationships between refinery corrosivity and chemical properties of sulfur and organic acid species has been performed. The corrosion tests of model oil mixtures as well as virgin Athabasca bitumen were carried out in a test unit that simulates corrosion found in refinery vacuum distillation towers. The results show that not only content but molecular weight and structure of the acids, and the structures of sulfur species influence high temperature corrosion. These factors need to be considered to improve the reliability of petroleum corrosivity assessment.

ACKNOWLEDGEMENTS

First, I would like to extend my gratitude to my supervisors Dr. Heather Dettman and Dr. Jingli Luo for their guidance, support and encouragement throughout my graduate program and research.

I would like to thank my group members in particular: Dr. Louis Heerze, Sara Salmon, Albert Chan and David Zinz for valuable conversations, as well as Norma McLean, Lindsay Logan and Dhanuka Wickramasinghe for lab assistance. I would also thank the CETC-Devon analytical group (Denis, Andrew, Cecile, and Anna) for performance of TAN and high temperature simulated distillation analyses, Vicente Muñoz and Dr. Glen Elliott for collecting the SEM pictures, and the Analytical Services Group in the Department of Chemistry at the University of Alberta for elemental analyses (C, H, N, S, O).

I would like to acknowledge financial support from the Alberta Science and Research Authority (COURSE/AERI) and the Canadian Association of Petroleum Producers (CAPP) through the Department of Chemical and Materials Engineering at the University of Alberta. As well, an in-kind contribution has been made by Natural Resources Canada (NCUT and CETC-Devon), through partial funding by the Canadian Program for Energy Research and Development, the Alberta Research Council and the Alberta Energy Research Institute.

Finally, thanks to my dearest family, whose unflinching love and support has always encouraged me.

TABLE OF CONTENTS

LIST OF TABLES

LIST OF FIGURES

LIST OF SYMBOLS AND ABBREVIATIONS

A	pre-exponential factor
AET	atmospheric equivalent temperature
ATHB	Athabasca bitumen
ATHBA	organic acids Isolated from Athabasca bitumen
b.p.	boiling point
C	sulfur concentration
C_0	initial sulfur concentration
C-C	carbon-carbon
CMNA	commercial naphthenic acid
CR	corrosion rate
CS	carbon steel
C-S	carbon-sulfur
D	diameter of pipe
E_a	activation energy
EDX	energy dispersive X-Ray
e/D	relative roughness
f	friction factor
FT-IR	fourier transform infrared spectra
GC	gas chromatography
HTSD	high-temperature simulated distillation
HVGO	heavy vacuum gas oil
k	apparent rate constant
kPa	kilo Pascal
LVGO	light vacuum gas oil
μ	dynamic viscosity
m.p.	melting point

MW	molecular weight
n	apparent reaction order
NMR	nuclear magnetic resonance
psi	pound per square inch
R	ideal gas law constant
R_e	Reynold's number
s	corrosion area
SCD	sulfur chemiluminescence detection
SEM	scanning electron microscope
SS	stainless steel
S-S	sulfur-sulfur
T	temperature
t	duration
τ	shear stress
TAN	total acid number
V	velocity of fluid
VR	vacuum residue
Δw	weight differences
ρ	density

Chapter 1. Introduction

1.1 Background and Motivation

High temperature corrosion, first investigated in the 1950's [1] continues to cause reliability issues in refineries [2]. The main cause of high temperature corrosion was identified to be due to organic acids present in the crude oil, generally called naphthenic acids. However, sulfur species are also known to cause corrosion. Consequently the relative contributions of organic acids and sulfur species should be considered. However, most references in the literatures discussed these problems separately before the mid-1990's.

Crudes containing higher contents of organic acids and sulfur are often referred to as "opportunity crudes" because they can be purchased at discounted prices. [3] However the economic loss due to high temperature corrosion in the refinery can be enormous. For example, a typical discount for an opportunity crude is from $1.00 to $3.00 less per barrel than that of benchmark crudes. Consequently, a profit of $200,000 to $600,000 can be made quickly in an average refinery having a throughput of 200,000 bbl/day [4-6]. However, profits can only be realized on the long term if effective techniques to control or prevent corrosion are implemented.

Typically, the corrosion engineer has only a few weeks to decide on how to process the opportunity crude safely. At best, the decision is based on a crude assay including total acid number (TAN) and sulfur content of distillation cuts. Corrosion mitigation approaches include adjusting the blending ratio of opportunity crude to quality crude for refinery feedstock, adding a corrosion inhibitor, or changing process conditions. The decisions are often based on previous experience, if any, and simple "rules of thumbs" using TAN and sulfur content. However, it is now realized that many of these rules are not reliable in their predictive ability [7]. Other factors such as, molecular weights and structures of the organic acids, structures of the sulfur species

relative to their thermal stability, and the interaction of organic acid and sulfur species are not usually considered.

After the mid-1990's, research on the synergy of organic acids and sulfur species with respect to high temperature corrosion increased [8-13]. Variables such as flow conditions and sulfur species were beginning to be considered. Nevertheless, there are still many deficiencies in the understanding of the interactions between these corrosive agents.

1.2 Organic Acids and High Temperature Corrosion Mechanism

Generally, the term "naphthenic acid corrosion" is used to account for all corrosion problems caused by organic acids present in crude oil at high temperature. However, the term "naphthenic acid" is derived from the early discovery of monobasic carboxylic acids in petroleum, where these acids consisted of a saturated single-ring structure [7]. Later, more extensive laboratory studies revealed a large variety of organic acids to be present in crude oil [19]. These included straight and branched chain carboxylic acids as low in molecular weight as formic and acetic acids. As well, the acids could include from one to six rings, saturated and/or unsaturated [1]. In this thesis, organic acid is a generic name used for the carboxylic acids with the chemical formula RCOOH where R can include chain and/or ring structures [14]. Organic acids are most active at temperatures above or at their boiling points and the most severe corrosion generally occurs when they condense on the metal surface. The corrosion formula can be written as [16]:

$$2RCOOH + Fe \rightarrow Fe(RCOO)_2 + H_2 \qquad (1.1)$$

The normal corrosion product of organic acids is an oil-soluble iron naphthenate that produces characteristic grooves on the surface of the metal. In a system containing both hydrogen sulfide and organic acids, there may be competition between the formation of iron naphthenate and iron sulfide.

As iron sulfide is oil-insoluble, it tends to form a film on the metal surface. This film can accumulate on surfaces during low-velocity conditions, and can protect the surface from organic acid corrosion. Increasing organic acid concentrations appear to first damage the integrity of the sulfide film and then, at higher acid concentrations destroy it. The classical model characterizes the corrosion mechanism in the presence of H_2S as the three competing reactions given in equations (1.1, 1.2 and 1.3) [16]:

$$Fe + 2RCOOH \rightarrow Fe(RCOO)_2 + H_2 \quad (1.1)$$

$$Fe + H_2S \rightarrow FeS + H_2 \quad (1.2)$$

$$Fe(RCOO)_2 + H_2S \rightarrow FeS + 2RCOOH \quad (1.3)$$

1.3 Refinery Distillation System and Risk Assessment

An illustration of the processes involved during petroleum distillation in refineries is shown schematically in Figure 1.1. The oil is preheated by heat exchangers using, for example, hot product streams from the process. It is then passed through the furnace tubes which supply the remaining heat requirement by direct firing. The oil is then transferred to the atmospheric distillation column. Here the lighter products (i.e. boiling point (b.p. up to 343°C) are distilled. The heavy hydrocarbon residue remaining at the bottom of the column is transferred to the vacuum distillation column through another heating system. In Figure 1.1, the second column operates under vacuum, permitting distillation of petroleum species with boiling point range between 343°C and 524°C without cracking (actual temperature below 343°C). The conditions, such as temperature, pressure and flow rate, vary along the system units so the impacts of corrosion vary along the refinery system.

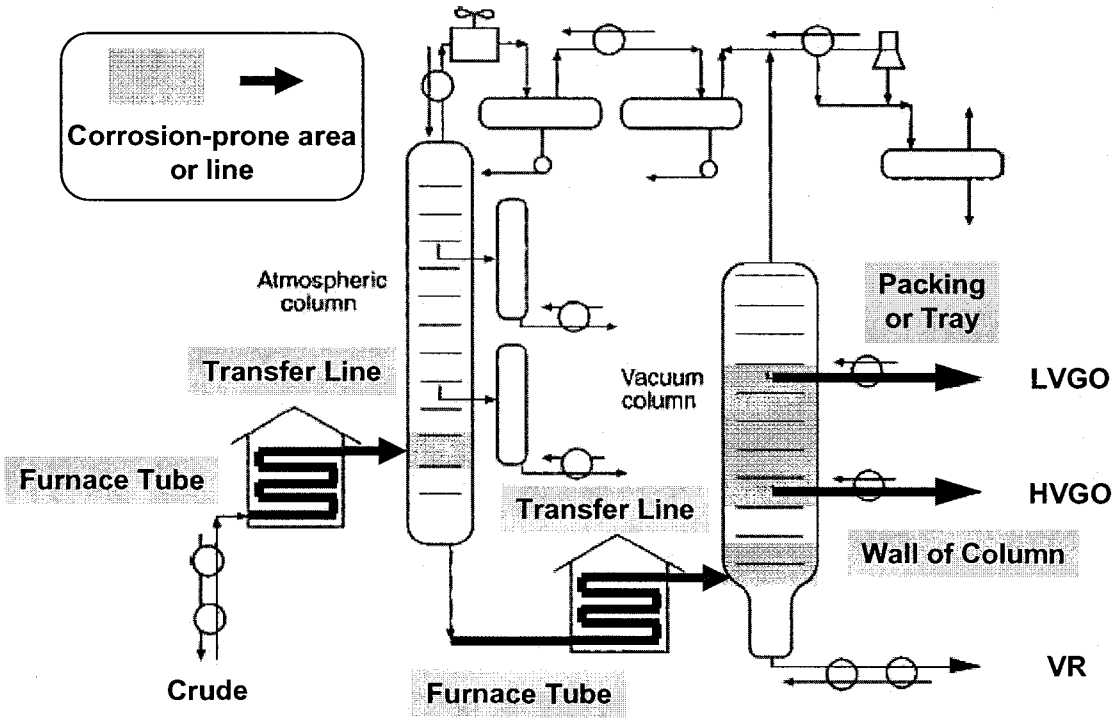

Figure 1.1 Schematic Diagram of Refinery Distillation System

To safely run crude oils in refineries, it is important to first assess the susceptibility of the plant and equipment to undergo high temperature corrosion. Typically, corrosion coupon data are reviewed to establish potential corrosion rates that are then used to estimate the remaining life of the process units, pressure pipelines, pumps and vessels.

Published literature [15-19] and experience indicate that pipelines and equipment containing crude, diesel (b.p.: 150~380°C), atmospheric residue (b.p. +343°C), light and heavy vacuum gas oil (b.p.: 343~524°C) and vacuum residue (b.p. +524°C), operating at temperatures higher than 220°C are possible areas for organic acid attack. The shaded areas in Figure 1.1 indicate the locations that can be affected. The most frequent locations for organic acid corrosion problems are in the furnace and transfer lines [14]. Other equipment typically affected includes pumps, heater tube inlets, return bends, heat exchangers and towers [15].

Unfortunately, experience has shown that it is difficult to correlate corrosion rates for any particular crude from refinery to refinery. This is due to differences in

equipment design including operating temperature, flow velocities and use of crude blends.

1.4 Parameters Affecting High Temperature Corrosion

There are several important factors [16-22] that have been identified to contribute to the corrosivity of crude, including TAN, acid molecular structure, sulfur content, process parameters (resident time, temperature and local flow conditions), and metallurgy [23-38]. Some of the factors have been extensively studied, yet limited progress has been achieved toward the understanding of corrosivity. The influence of each factor is often difficult to be identified because these parameters are interdependent.

1.4.1 Total acid number

The total acid number is defined by the American Society for Testing and Materials (ASTM) as the quantity of base, expressed as milligrams of KOH required to neutralize the acidic components in 1 g of oil. It is a measure of all acidic components in the oil, including organic acids and non-organic acids. Common practice in oil refineries is to use TAN [39, 40] as a measure of crude corrosivity. Historically, crudes with low TAN values have been considered "safe" for refinery processing, whereas those with TAN values above arbitrary limits are considered to be corrosive. For example, crude oils with TAN values higher than 0.5 mg KOH/g and distillate fractions with TAN values higher than 1.5 mg KOH/g are considered to be corrosive. Some references suggest that the critical TAN should be between 0.5 and 2.0 mg KOH/g oil [8]. However, there usually is poor correlation between TAN values and the corrosivity of crude oils [41,42]. Experience has shown that organic acids vary in their structure and molecular weight between crude oils, even if the TAN values are the same. Such differences suggest that there is the need to understand the relationship between organic acid structure and size, and corrosivity.

1.4.2 Sulfur content

Some oils possess "corrosion inhibiting" qualities [40]. It has been proposed that the inhibition is a result of the sulfur present in the oil as H_2S, or as compounds that convert to H_2S, because the usual product of H_2S corrosion is an oil- insoluble iron sulfide (FeS). The precipitated iron sulfide can form a protective layer for the metal. Organic acids, in contrast, form oil-soluble iron naphthenates. It is suggested that in the presence of both organic acids and H_2S, the rate of organic acid corrosion decreases due to iron sulfide protection of the metal. The relationships between organic acid (RCOOH), hydrogen sulfide (H_2S) and iron (Fe) are showed in Figure 1.2

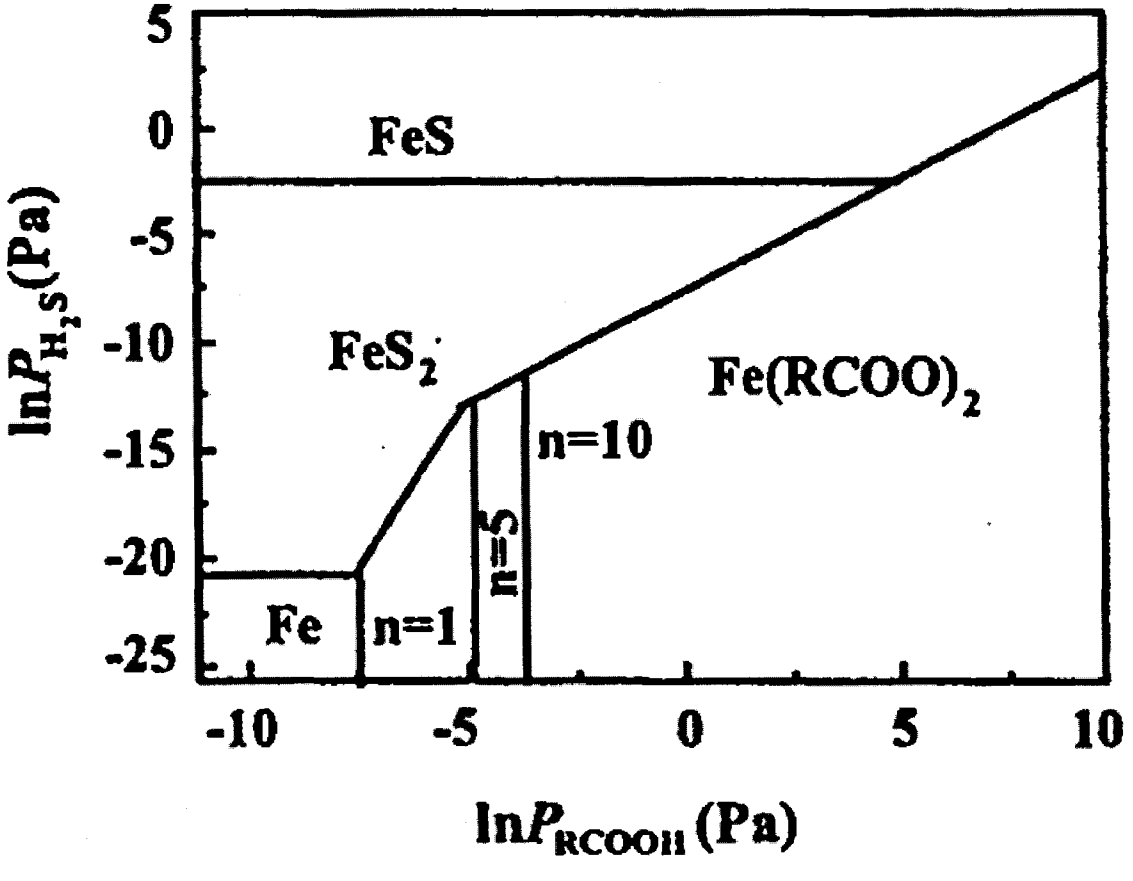

Figure 1.2 Phase Diagram for the RCOOH- H_2S-Fe System Where n is the Carbon Number of the Acid [60]

There is a non-corrosion area (Fe), a corrosion inactivation area (FeS) and a corrosion area ($Fe(RCOO)_2$). The graph shows several features. Firstly, there exists, a critical pressure in reaction of organic acids with iron below which corrosion will not occur. Secondly, the partial pressure of H_2S influences both the formation of the iron sulfide film and its ability to resist corrosion. Finally, as the carbon number of the acid (n) increases, the critical pressure increases, and the organic acid corrosion decreases [60]. Despite higher H_2S content generally being considered beneficial for the inhibition of organic acids attack, increased concentrations of reactive sulfide may trigger high temperature sulfidic corrosion. And traditional metallurgies that are resistant to high temperature sulfidic corrosion are not very resistant to high temperature organic acid corrosion attack.

Just as the correlation between TAN values and the organic acid corrosion is inconsistent, the correlation between total sulfur content and sulfidic corrosion is inconsistent. H_2S is known to be the main corrosive agent of sulfidic corrosion. Consequently information about the thermal cracking behavior of different sulfur compounds to H_2S under refinery thermal conditions is needed to understand the relationship between the sulfur types (i.e. mercaptans, sulfides and polysulfides) content and structure, and corrosivity [42].

1.4.3 Processing parameters

In addition to crude corrosivity, the temperature of the oil has a great influence on the corrosion rate [43-46]. For example, organic acid corrosion is normally not a concern below 220°C. As temperature increases, the corrosion rate tends to increase until 400°C where the organic acids begin to crack. However the specific relationship between corrosion rate and temperature is not fully understood. Gutzeit reported the results of field surveys that corrosion of most steels approximately triples with each 55°C increase [43]. He suggested that the corrosion kinetics can be represented by an Arrhenius-type equation at temperatures >288°C, with an activation energy of 68.5 kJ/mol.

High temperature sulfidic corrosion usually occurs in process units at temperatures above 260°C [47]. The "Couper–Gorman" curves provide a reasonably

good prediction tool for high temperature systems containing hydrogen [48]. "McConomy curves" [49, 50] are commonly used to predict the relative corrosivity of crude oils and their various fractions when negligible hydrogen is present.

Both the organic acid corrosion and sulfidic corrosion are sensitive to flow velocity, the local turbulence, and degree of vaporization [43, 44, 51]. Wall shear stress most accurately accounts for these factors because it includes the density and viscosity of liquid and vapor in the pipe, the degree of vaporization in the pipe, and the pipe diameter. However, no quantitative relationship between corrosion rate and wall shear stress has been developed

1.4.4 Alloy type

Different materials have different abilities to resist organic acid corrosion. Table 1.1 gives the corrosion rates of a variety of alloys in a crude unit vacuum column [52]. This test, run at 271°C and with a crude TAN of 3.9 mg KOH/g, demonstrates the importance of molybdenum and chromium in assuring good resistance to organic acid corrosion. Consequently, normal construction materials used in crude distillation units are ranked according to the organic acid corrosion resistance from low to high as: carbon steel; 5Cr1/2Mo and 9Cr1Mo low alloy steels; 410; 304; 316 and 317 stainless steels.

Table 1.1 Corrosion Rate of Different Alloys in a Crude Unit Vacuum Column [52]

Material	Content of Cr	Content of Mo	Corrosion rate (mm/y)
Carbon steel	Nil	Nil	0.68
AISI 410 SS	11.5-13.5	Nil	0.53
AISI 430 SS	12.5-14.5	Nil	0.26
AISI 304 SS	18~20	Nil	0.37
AISI 316 SS	16~18	2~3	<0.001
AISI 317 SS	16~18	2~3	<0.001
Incoloy 800	19~23	Nil	0.26
Inconet 600	14~17	Nil	0.43

For sulfidic corrosion, according to the modified McConomy Curve used by Cataldi *et. al.* [50,53], corrosion rates are roughly halved when the next higher grade of low-alloy steel is selected. Both the curves and the data in Table 1.3 demonstrate the beneficial effects of alloying element chromium and molybdenum on reducing corrosion rates. However it does not provide details about roles of alloying elements in combating against organic corrosion and sulfidic corrosion.

1.5 Control of High Temperature Corrosion

High temperature corrosion can be controlled by blending crudes with different TAN value, corrosion inhibitors, use of corrosion-resistant alloys and process conditions [54-57]. Blending may be used to reduce the organic acid concentration content of the feed by diluting high TAN crude with low TAN crude, thus reducing corrosion rate to an acceptable level. Blending is also used to increase the sulfur content in the feed to inhibit organic acid corrosion. Control of organic acid corrosion by chemical additives as inhibitors has been studied recently where phosphorus-based

corrosion inhibitors have been found to be effective at high temperatures. Injection of corrosion inhibitors may provide protection for specific fractions that are known to be particularly corrosive. For long-term reliability, upgrading the construction materials to a higher chrome and/or molybdenum alloy is the best solution. Among the corrosion-resistant alloys, molybdenum-containing stainless steels like AISI 316 and 317, or aluminized steel were found to be effective in high temperature environments [58, 59].

1.6 Research Objective

In the present study, the influences of variables such as duration, temperature, and materials on organic acid corrosion were examined. Particular emphasis was placed on properties of the organic acid and the interaction of organic acid and sulfur compounds. This information will contribute to the understanding of high temperature corrosion in oil refining environments.

A fundamental study of the relationships of chemical prosperities, such as molecular structures and molecular weight of organic acids to corrosivity has been performed. In particular, the corrosiveness of homologous series of organic acid compounds with respect to temperature has been assessed in a test unit that simulates corrosion found in refinery vacuum distillation towers.

To improve the understanding of sulfidic corrosion, two types of studies were performed. First, the decomposition behavior with temperature of sulfur species was determined for model sulfur compounds chosen to represent different types of sulfur-carbon bonds. Secondly the corrosivity of selected sulfur compounds was determined.

The corrosivity of the model compounds were then compared to that of Athabasca bitumen. Both the virgin bitumen and its extracted organic acids dissolved in white oil were compared.

1.7 Thesis Overview

The remainder of the thesis is organized as follows:

Chapter 2 describes the study variables of organic acid corrosion in the absence of sulfur. Particular emphasis was placed on the influence of molecular weight, structure, and boiling point on corrosivity.

Chapter 3 describes the thermal stability of sulfur compounds under refinery conditions in order to understand the range of H_2S formation possible from different sulfur compounds during refinery thermal conditions and residence times.

Chapter 4 describes the study of the influence of different types and content of sulfur compounds on organic acid corrosion and evaluates the performance of different materials.

Chapter 5 describes the study of corrosivities of Athabasca bitumen and its isolated organic acids dissolved in white oil. The results are compared with those obtained for a commercial naphthenic acid dissolved in white oil.

Chapter 6 provides conclusions and future directions for this work.

1.8 References

[1] H.A.*Cataldi*, R.J. Askevold and A.E. Harnsberger, Petroleum Refiner, Vol. 32, No. 7, p. 145, (1953)

[2] S. Tebbal, Corrosion 1999, NACE Paper No. 380, (1999)

[4] S. Tebbal, Corrosion 2004, NACE Paper No. 04636, (2004)

[5] S.A.Bradford, Corrosion control, 2nd Edition, CASTI Publishing Inc., Edmonton, Alberta, Canada, p. 4 (2001)

[6] "Canada 's Energy Markets: Sources, Transformation and Infrastructure", Natural Resources Canada, <www2.nrcan.gc.ca/es/ener2000/online/html/chap3f_e.cfm> (June 14, 2006).

[7] S. Tebbal and R. Kane, Corrosion 1998, NACE Paper No. 578, (1998)

[8] N.R. Smart, A.P. Rance, A.M. Pritchard, Corrosion 2002, NACE Paper No. 02484, (2002)

[9] R.D. Kane, M.S. Cayard, Corrosion 2002, NACE Paper No. 02555, (2002)

[10] F.W.H.Dean, Corrosion 2002, NACE Paper No. 02344, (2002)

[11] K.R. Lewis, M.L. Daane, Corrosion 1999, NACE Paper No. 377, (1999)

[12] Jonathan D. Dobis, Corrosion 1997, NACE Paper No. 510. (1997)

[13] M.J. Nugent, J.D. Dobis, Corrosion 1998, NACE Paper No. 577, (1998)

[14] Hopkinson, B. E., Penuela, L. E., Corrosion 1994. NACE Paper No. 531, (1994)

[15] Breen, A. J., Br. Corros. (Quarterly), Vol. 9, No. 4, p. 197 (1974)

[16] E. Slavcheva, B. Shone and A. Turnbull, Br.Corrossion. J, Vol. 34, No. 2, p. 125, (1999)

[17] R.D. Kane and M.S. Cayard, Hydrocarb. Processing, Vol.74, No11, p. 129, (1995).

[18] W. P. Jepson, Corrosion 1997. NACE Paper No. 11, (1997)

[19] Michael V. Enzien, Corrosion 1996, NACE Paper No. 290, (1996)

[20] E. Slavcheva, B. Shone, A. Turnbull, Corrosion 1998, NACE Paper No. 579, (1998)

[21] H.J.d. Bruyn, Corrosion 1998, NACE Paper No. 576, (1998)

[22] G.L. Scattergood, R.C. Strong, W.A. Lindley, Corrosion 1987, NACE Paper No.197, (1987)

[23] B.E. Hopkinson, L.E. Penuela, Corrosion 1997, NACE Paper No. 502, (1997)

[24] H. L. Craig, Corrosion 1995, NACE Paper No. 333, (1995)

[25] J.H. Lee Craig, Corrosion, 1996, NACE Paper No. 603, (1996)

[26] H. Simon, Corrosion, 1979, NACE Paper No. 29, (1979)

[27] R.L. Piehl, Corrosion, 1987, NACE Paper No. 196, (1987)

[28] A. Turnbull, E. Slavcheva and B. Shone, Corrosion, Vol. 54, No. 11, p. 922. (1998)

[29] G.C. Laredo, C.R. Lopez, R.E. Alvarez and J.L. Cano, Fuel, Vol. 83, No.11, p. 1689, (2004)

[30] B. Messer, B. Tarleton, M. Beaton, T. Phillips, Corrosion 2004, NACE Paper No. 04634, (2004)

[31] B.F. Qi, X. Fei, S.J. Wang and L.R. Chen, Pet. Sci. Technol. Vol. 22, No.3–4, p. 463, (2004)

[32] M.P. Barrow, L.A. McDonnell, X.D. Feng, J. Walker and P.J. Derrick, Anal. Chem. Vol.75, No. 4, p. 860, (2003)

[33] X.Q. Wu, H.M. Jing, Y.G. Zheng, Z.M. Yao and W. Ke, Wear, Vol. 256, No. 1–2, p. 133, (2004)

[34] X.Q. Wu, H.M. Jing, Y.G. Zheng, Z.M. Yao and W. Ke, Mater. Corros. Vol. 53 No. 11-12, p. 833, (2002)

[35] D.R. Qu, Y.G. Zheng, H.M. Jing, X. Jiang and W. Ke, Mater. Corros. Vol. 56, No. 8, p. 1, (2005).

[36] N.R. Smart, A.P. Rance, A.M. Pritchard, Corrosion 2002, NACE Paper No. 02484 (2002)

[37] A.M. Pritchard, A. Graham, A. Rance, Corrosion 2001, NACE Paper No. 01525, (2001)

[38] D. Johnson, G. McAteer, H. Zuk, Corrosion 2003, NACE Paper No. 03645, (2003)

[39] R. L. Piehl, Corrosion 1987, NACE Paper No. 196, (1987)..

[40] A. Groysman, Corrosion 2005, NACE Paper No. 05568, (2005)

[41] E. Babaian-Kibala, H.L. Craig, G.L. Rusk. Rusk. K.V. Blanchard. T.J. Rose. B.L. Uehlein. R.C. Quinter. M.A. Summers, New Orleans, LA, USA Vol. 93 Paper 631, p. 50, (1993)

[42] E.A. Bardaz, Proceeding 6th European Conference on Corrosion Inhibitors, Italy, (1985)

[43] J. E. Slater, Director of Refining, API. API Publication 943, p. 45, (1974).

[44] J. L. Hau, O. Yepez, M. I. Specht and R. Lorenzo, Corrosion 1999, NACE Paper No. 379, (1999)

[45] A. Bagdasarian, J. Feather, B. Hull, R. Stephenson and R. Strong, Corrosion 1996, NACE Paper No. 615, (1996)

[46] B. Batra, C. A. Borchert, K. R. Lewis, A. R. Smith, Chemical Engineering Progress, p. 68, (1993)

[47] A. Jayaraman and R.C. Saxena, Corros. Prev. Control, Vol. 42, No. 6, p. 123, (1995)

[48] A.S. Coupper and J.W. Gorman, Mater. Protect. Perform, Vol. 10, No. 1, p. 31, (1971)

[49] K.C. Baker, Mater. Perform. Vol. 40, No.5, p. 62, (2001)

[50] R.D. Kane and M.S. Cayard, Hydrocarb. Process. Vol. 77, No. 10, p. 97, (1998)

[51] M.J. Zetlmeisl, Corrosion, 1995, NACE Paper No. 334, (1995)

[52] X.Q. Wu, H.M. Jing, Y.G. Zheng, Z.M. Yao and W. Ke, Corrosion Science, Vol. 46, No. 4, p. 1013, (2004)

[53] H.A.Cataldi, R.J. Askevold and A.E. Harnsberger, Petroleum Refiner, Vol. 32, No. 7, p. 145, (1953)

[54] Blanco, E. F, and Hopkinson, B, Corrosion 1983, NACE Paper No. 99, (1983).

[55] E. Mirabal and C. Molina, Corrosion 1999, NACE Paper No. 80, (1999)

[56] J.I. Danis and A.C. Gysbers, Corrosion1998, NACE Paper No. 589, (1998)

[57] E. Babaian-Kibala, P.R. Petersen, M. J. Humphries, American Chemical Society meeting, March 29-April 3, 1998, Dallas, Texas.

[58] M. J. Zetlmeisl, Corrosion 1996, NACE Paper No. 218, (1996).

[59] C. Shargay, and D. Cobb, Fifteenth World Petroleum Congress, Beijing, China, October (1997)

[60] Y. Gao, Journal of Chinese Society for Corrosion and Protection, Vol.19 No.6, p. 56, (1999)

Chapter 2. Influence of Chemical Properties on Organic Acid Corrosion

2.1 Introduction

Generally, an increase in TAN is accompanied by an increase in refinery corrosion rate [1,2]. Under the classical model, crude oils with TAN values greater than 0.5 mg KOH/g and distillate sub-fractions with TAN values over 1.5 mg KOH/g are considered to be corrosive [2,3,4]. However, it is not uncommon to observe significant differences in corrosivity between crude oils that have the same value of TAN [5, 6]. For example, Canadian Athabasca oil sands bitumen is predicted to be corrosive by the classical model. However, after more than 50 years of cumulative operation, upgraders have experienced negligible organic (naphthenic) acid corrosion [7].

A possible explanation for this discrepancy may be found in differences in chemical compositions and properties of the organic acids found in crude oils including their structure, boiling point and molecular weight [8-13]. Zetlmeisl *et. al.* have shown that the classical model for organic acid corrosion is inadequate for predicting refinery corrosion due to its assumption that all acid molecules are equally corrosive regardless of their composition and structure [14]. Derungs had mentioned as early as 1956, that molecular sizes and structures of the organic acids will influence corrosion [2]. However, the correlation between corrosivity and molecular structure is still ambiguous.

In the present study, a corrosion unit has been developed to simulate corrosion found in refinery vacuum distillation towers. Variables of organic acid corrosion, such as time, temperature, TAN, and chemical structures have been studied, specially the influence of the chemical properties of organic acids on corrosivity.

Model oil mixtures were prepared using individual organic acid compounds dissolved in white oil where the organic acid compounds contained various carbon and ring numbers. Model oil mixtures in white oil were also prepared using a commercial naphthenic acid mixture.

2.2 Experimental Procedures

2.2.1 Materials and media

The eleven organic acid compounds chosen for this study are shown in Table 2.1. These compounds and the commercial naphthenic acid were purchased from Sigma Chemical Company (3050 Spruce street, St. Louis, MO 63103). The white oil (Klearol mineral oil with negligible acid or sulfur content, boiling point [b.p.] 227-512°C) was purchased from Acatris Inc (2770 Portland Drive, Oakville, Ontario L6H6R4). Carbon steel 1018 coupons were purchased from Caproco (4815 Eleniak Road, Edmonton, Alberta, Canada T6B2N1).

All model oil mixtures with individual organic acid compounds were prepared to a TAN value of approximately 5.0 mg KOH/g and the model oil mixtures containing commercial naphthenic acid were prepared to TAN range from 0.5 to 5.0 mg KOH/g. The TAN values were confirmed using the CCQTA-modified ASTM method D-664 in units of mg KOH/g of oil.

Carbon steel test specimens were machined as rectangular coupons with dimension of 1"× 1/2" × 1/8". An off-centered hole of 1/2" diameter was made to permit hanging them on glass hooks in the corrosion test unit. Both before and after corrosion tests coupons were cleaned sequentially with toluene and acetone three times, dried with nitrogen, and weighed [16].

Table 2.1 Organic Acids Used in Model Oil Mixtures

Name	MW	B.P.	Structure
Hexanoic acid	116.16	202-203 °C	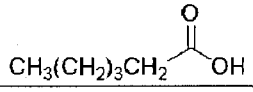
Benzoic Acid	122.12	249 °C	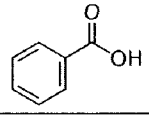
Cyclohexanecarboxylic acid	128.17	232-233 °C	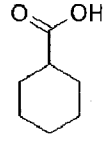
1,2,3,4-Tetrahydro-2-naphthoic acid	148.20	299°C	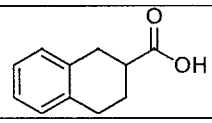
3-Cyclohexanepropionic acid	156.22	276 °C	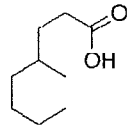
4-Phenylbutyric acid	164.20	307°C	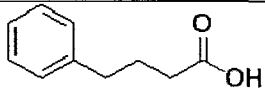
Cyclohexanebutyric acid	170.25	303 °C	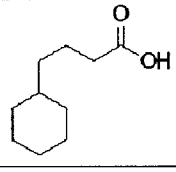
1-Naphthoic acid	172.18	300 °C	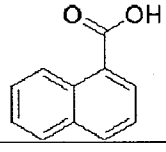
5-Acenaphthenecarboxylic acid	198.22	220°C (m.p.)	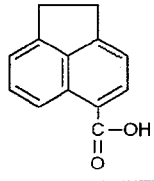
Fluorene-1-carboxylic acid	210.23	246°C (m.p.)	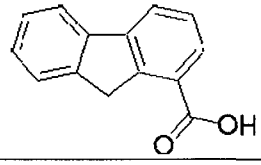
Stearic acid	284.48	361°C	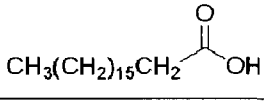
Commercial naphthenic acid			b.p.: 165-567°C

2.2.2 Corrosion unit description

The corrosion test unit used for this study is shown in Figure 2.1 and was designed to simulate corrosion activity in a vacuum tower where both liquid and vapor phase corrosion environments exist. The apparatus includes a 500 mL round bottom flask, a still column and a condenser. There are three systems connected to the apparatus: heating through the mantle holding the round bottom flask; cooling of the overhead gases by the condenser filled with recycled ethylene glycol (temperature set to -20°C); and a nitrogen gas supply for flushing the system.

For each run, four test coupons were attached to the glass hooks and located in the flask and column: three coupons were above the liquid and so were exposed to vapor phase corrosion; and one was immersed in the liquid.

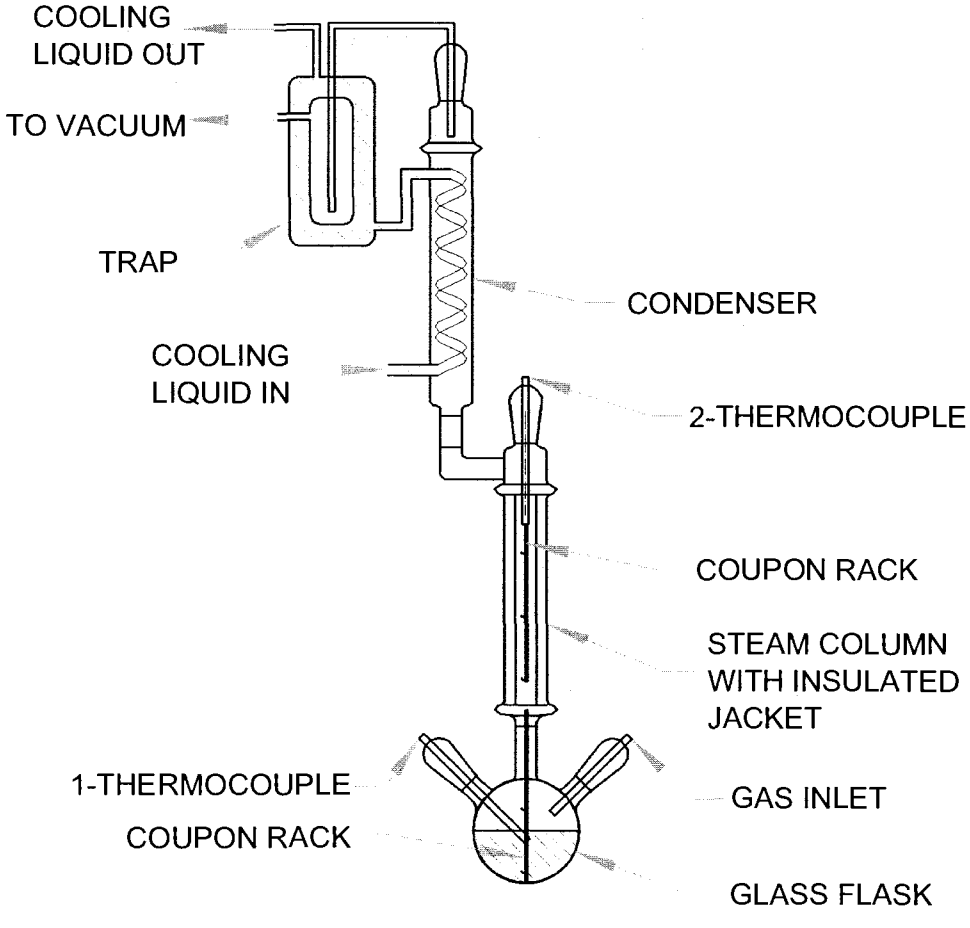

Figure 2.1 Schematic Diagram for the Corrosion Test Unit

2.2.3 Corrosion test method

The corrosion test unit was assembled and flushed with nitrogen to remove air. Vacuum was applied with a mechanical pump and regulated to desired pressure (between 100 and 300 mBar). The liquid (250 mL) was heated to the temperature required to meet the desired atmospheric equivalent temperature (AET) where pot temperatures ranged from 250 to 300°C[1]. The test duration ranged from 1 to 48 h and the corrosion rates (CR) in units of mm/y were calculated as follows:

$$CR = (\Delta w/\rho st) \times 24 \times 365$$

where: Δw (g) denotes the weight difference of specimens before the corrosion test and after the corrosion test with corrosion films being removed, ρ is the material density (g/mm^3), s is the corrosion area (mm^2), and t is the test duration (h).

All tests were carried out at least twice. The variability of results was within ±5 percent between the duplicate tests.

2.2.4 Microstructure analysis and morphology observation

A HITACHI S-2500 scanning electron microscope with INCAx-act energy dispersive x-ray spectroscopy (EDX) capability was used for morphology observation and composition analyses of coupon surfaces. Measurements were performed at room temperature using a 20 kV accelerating voltage.

2.3 Results

2.3.1 Influence of corrosion duration on corrosion

The model mixtures of commercial naphthenic acid in white oil (250 mL), with TAN approximately 5 mg KOH/g were tested at AET 300°C and 350°C forl h to 48 h. Table 2.2 lists the TAN value before and after the corrosion tests, as well as the mass

---

[1] For example, under the vacuum used, compounds with boiling points of up to 300°C would boil even though the actual temperature was 250°C.

balance of corrosion test unit during the runs. The corrosion rates are plotted as a function of time in Figure 2.2

Table 2.2 TAN Values and Test Unit Mass Balances with Time of Corrosion Tests (Initial TAN = 5.4 mg KOH/g)

Duration (h)	Final TAN (mg KOH/g)	Intial Weight of White oil (g)	Final Weight of White oil (g)	Mass balance (%)
1	5.2	251.19	250.98	99.9
2	4.9	250.78	250.56	99.9
4	4.5	251.24	250.76	99.8
8	2.4	250.98	249.53	99.4
48	0.2	251.10	248.65	99.0

The weight of the white oil, as a solvent in most of the corrosion tests decreased during the tests due to thermal cracking. This would affect the corrosion rate by introducing another variable if taking the weight loss of white oil into account during the test. The results from Table 2.2 show that the weight loss of white oil for the most severe condition is less than 1% so influence of white oil loss on the corrosion results are negligible.

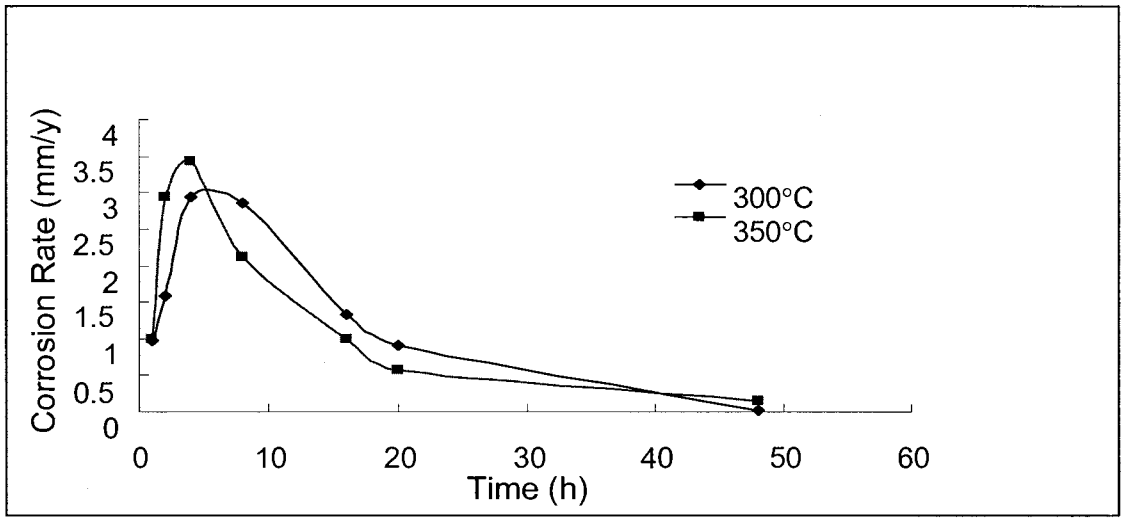

Figure 2.2 Corrosion Rates of Carbon Steel Coupons in Liquid with Time and AET

In Figure 2.2, the corrosion rates increased sharply between test runs of 1 h and 4 h duration, then the rates decreased gradually up to durations of 44 h. The initial increase with time indicates that acid damage is cooperative: as the metal surface becomes damaged, the metal becomes easier to damage. As the iron is removed from the metal, salts of the acid are formed and the TAN value decreased (Table 2.2). Table 2.2 also shows that the corrosion rate decreased. For the mixtures with TAN of 5 at AET values of 300°C and 350°C, the maximum corrosion rate was obtained at 4 h, consequently this test run time was chosen for most other corrosion tests.

2.3.2 Influence of TAN and temperature on corrosion

A set of model oils was prepared using commercial naphthenic acid in white oil having TAN values ranging from 0.5 to 5.0 mg KOH/g. Each mixture was tested for 4 h at three AET values, 300°C, 330°C and 350°C. The corrosion rates are plotted as a function of TAN in Figure 2.3

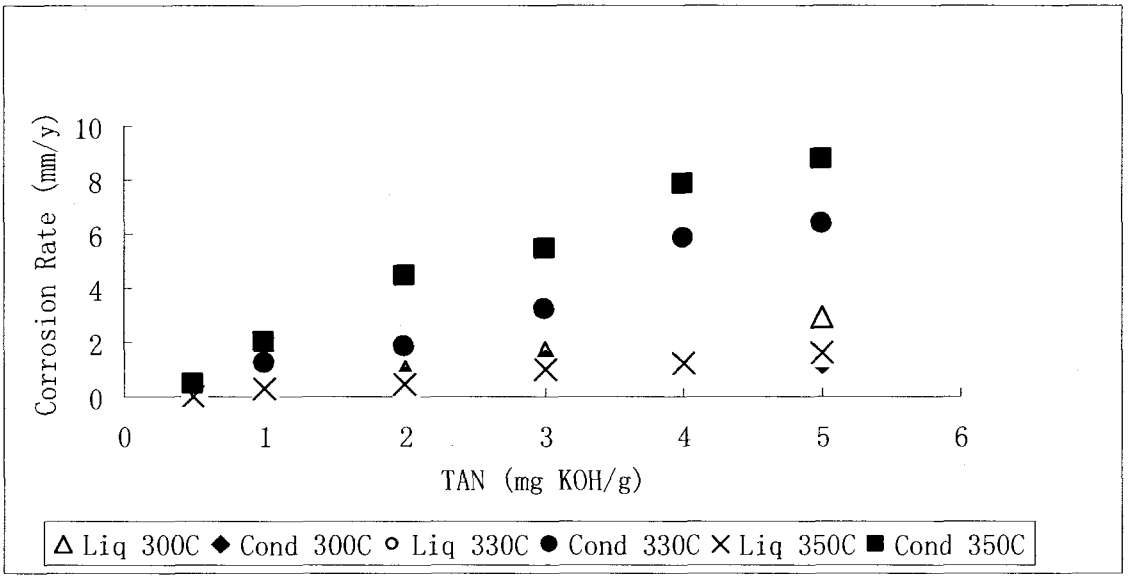

Figure 2.3 Corrosion Rates of Carbon Steel Coupons in Liquid (Liq) and Condensate (Cond) with TAN and AET

The results in Figure 2.3 show that the corrosion rates of carbon steel coupons increase with TAN and temperature, particularly for the coupons in vapor phase where the acids condense on the metal coupons (Condensate). At the higher AET values (330°C and 350°C), the corrosion rates of the coupons in the vapor environment are significantly higher than those in the liquids. This is consistent with corrosion behavior found in vacuum towers where high corrosion rates occur on metal surfaces when organic acid vapors condense and cause localized acid enrichment [18]. At lower AET values (300°C), corrosion rates due to condensate are lower because less organic acid is vaporized at that temperature. The results suggest that the corrosion rates of carbon steel coupons located in the condensate increase with TAN and temperature where as corrosion rates of those coupons immersed in the oil only increase with TAN value.

In Figure 2.4, electron micrographs show changes of surface morphologies with time of corrosion tests. Organic acid corrosion should result from general corrosion under these conditions which can be observed in Figure 2.4. However Figure 2.4 (b), (c) and (d) show that after 4 h, some grey or white dents called pits appear along scratch

lines on the surface (see arrows). This is particularly obvious at higher magnification Figure 2.4 (c), which indicates that selective corrosion also occurs. However the number and size of the pits did not increase significantly even after 48h corrosion test duration. [Figure 2.4 (d)]. The weight loss is mainly contributed to general corrosion.

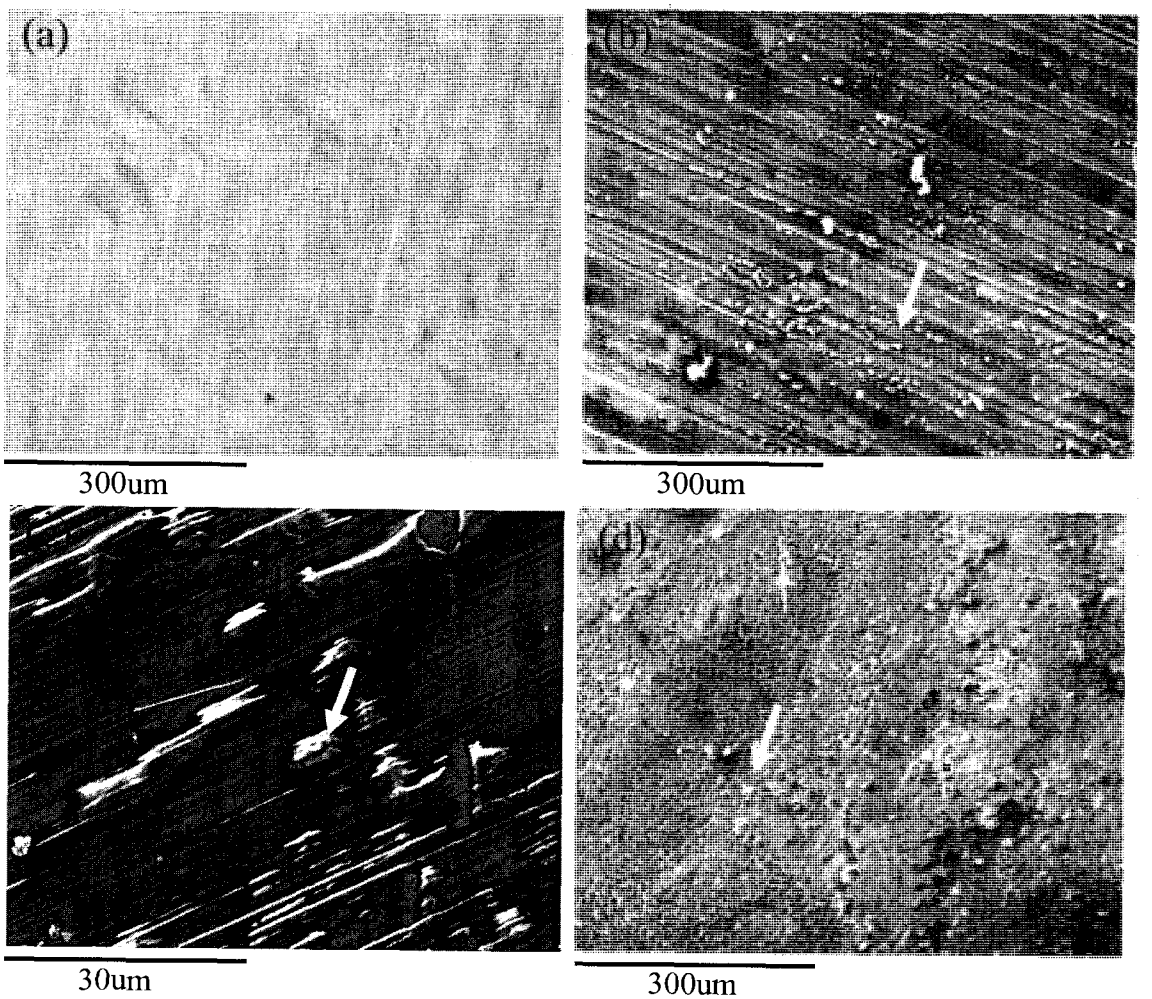

Figure 2.4 Electron Micrographs of Carbon Steel Coupons after Corrosion (TAN = 5 mg KOH/g) at (a)1 h, (b) 4 h, (c) high resolution of 4 h and (d) 48h

2.3.3 Influence of molecular weight, structure and boiling point of organic acids on corrosion

Model oil mixtures consisting of individual organic acid compounds in white oil were prepared to study the influence of chemical characteristics on corrosion rate. To minimize the number of experimental variables, each test mixture was adjusted to a TAN value of 5.0 mg KOH/g and was tested under the same temperature and vacuum conditions to achieve an AET value of 300°C. The corrosion rates of carbon steel coupons exposed to the eight model oil mixtures are shown in Figures 2.5 and 2.6.

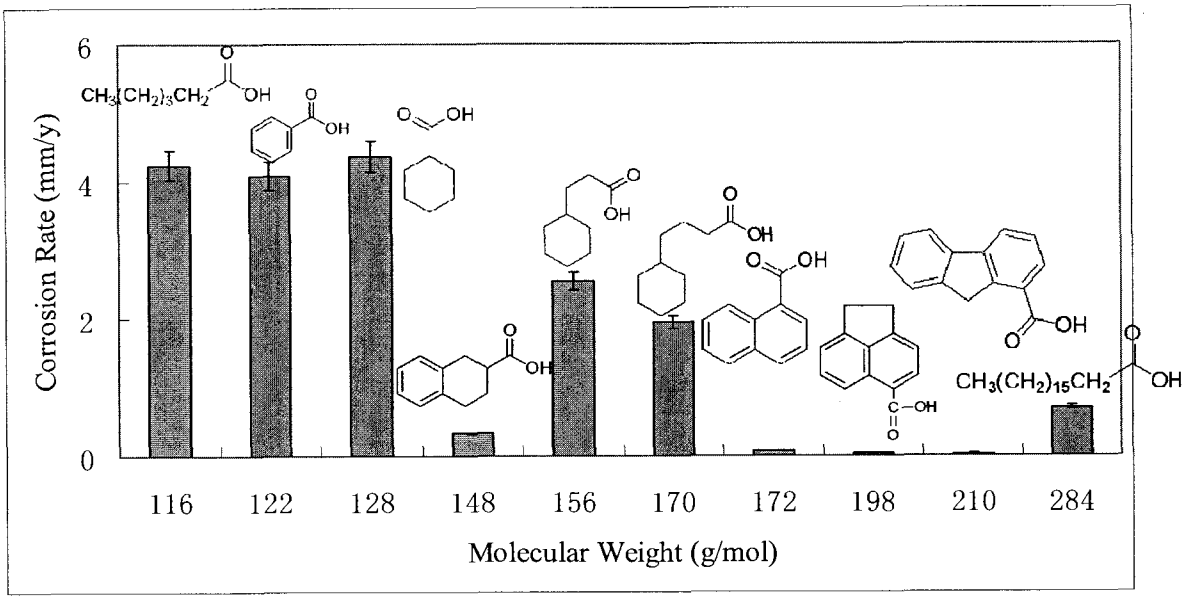

Figure 2.5 Corrosion Rates of Carbon Steel Coupons in Liquid of Model Oil Mixtures (AET = 300°C , TAN = 5.0 mg KOH/g)

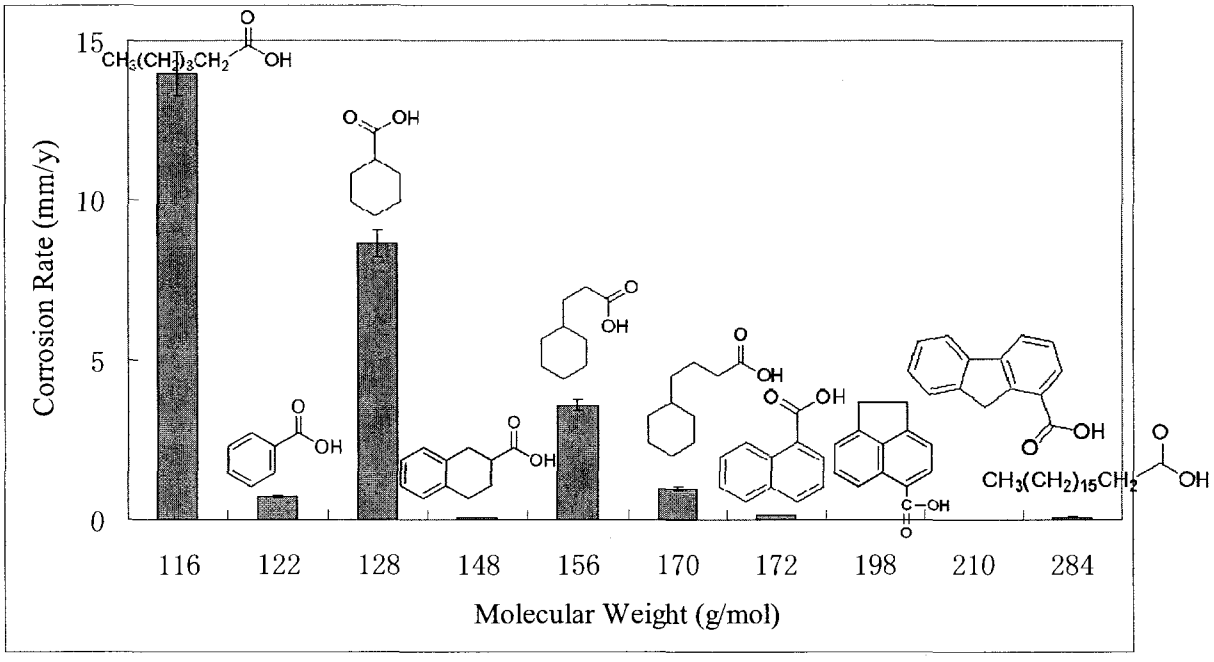

Figure 2.6 Corrosion Rates of Carbon Steel Coupons in Condensate of Model Oil Mixtures (AET = 300°C, TAN = 5.0 mg KOH/g)

The relationship of corrosion rates of carbon steel coupons immersed in the model oils and molecular weight is shown in Figure 2.5. The results indicate a tendency for the corrosion rate to decrease with molecular weight. This is particularly evident within homologous series (where the acid is written as RCOOH, and R is the same type of species but increase in size). For example, cyclohexanecarboxylic acid, cyclohexanepropionic acid and cyclohexanebutyric acid all consist of a cyclohexane ring with a chain terminal carboxylic acid group. For these three acids, as the molecular weight increased, the corrosion rate in the liquid decreased.

In Figure 2.6, the corrosion rates of carbon steel coupons in condensate of compounds in homologous series have similar trends to those found in the liquid. The corrosion rates decrease as molecular weights increase. For the light acid species, such as hexanoic acid, the corrosion rate is much higher in condensate than that in liquid.

Both Figure 2.5 and Figure 2.6 show that molecular structure also plays an important role in determining corrosivity. For example, cyclohexanebutyric acid and

1-naphthoic acid have similar molecular weights. However, cyclohexanebutyric acid with a single cycloalkane ring causes significantly greater corrosion of the carbon steel coupon in the liquid than 1-naphthoic acid with two aromatic rings. The corrosion rates for carbon steel coupons immersed in the oil decrease dramatically, when R contains more than one ring. This is illustrated by the corrosion rates of cyclohexanecarboxylic acid and benzoic acid when compared to those of 1,2,3,4-tetrahydro-2-naphthoic acid and 1-naphthoic acid in Figure 2.5.

The results indicate that organic acid corrosivity decreases as molecular weight and number of rings contained in the molecule increases: the smallest acid species with no ring structure were the most corrosive for carbon steel coupons placed both in the oil and in condensate

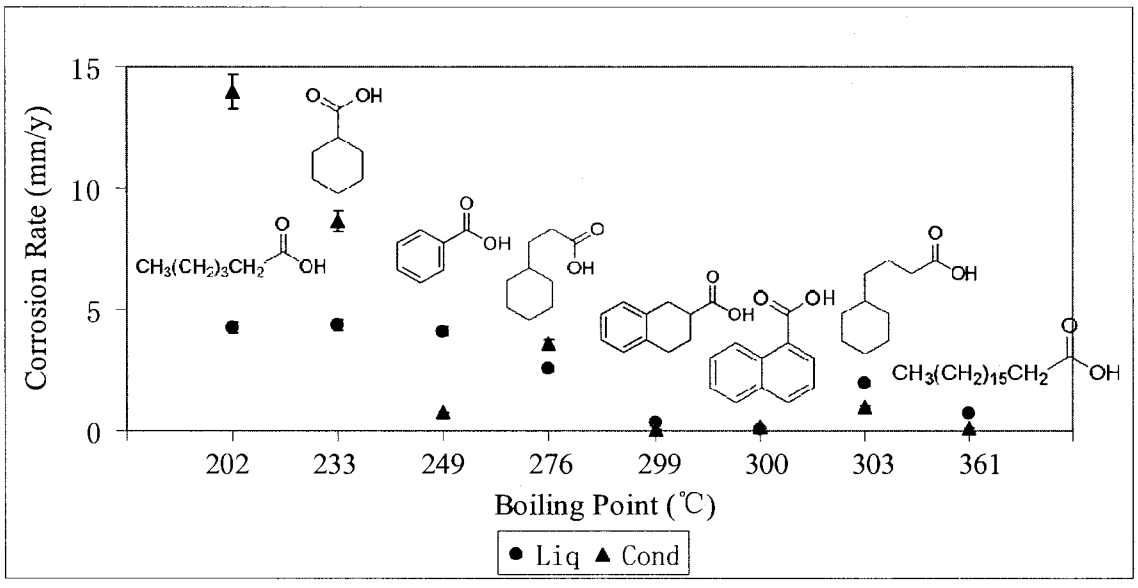

Figure 2.7 Corrosion Rates of Carbon Steel Coupons in Liquid (Liq) and Condensate (Cond) of Model Oil Mixtures (AET = 300°C , TAN = 5.0 mg KOH/g)

Figure 2.7 shows that the boiling point of the organic acid determines the threshold temperature at which corrosion in condensate begins. For the acid to cause corrosion in condensate, AET must be above the acid boiling point. Consequently, 1-naphthoic acid (b.p. 300°C), cyclohexanebutyric acid (b.p. 303°C) and stearic acid

(b.p. 361°C) had low corrosion rates because AET was close to or below their boiling points. When AET was above the organic acid boiling points, corrosion in condensate was observed where the corrosion rates again depended on the molecular weights and structures of the organic acids.

2.4 Discussion

2.4.1 Organic acid corrosion mechanism

As mentioned in Chapter 1 the organic acid corrosion reaction is generally described by:

$$Fe + 2RCOOH = Fe(RCOO)_2 + H_2 \qquad (1.1)$$

Equation (1.1) could apply both to chemical and electrochemical reactions [22]. It was generally accepted that organic acid corrosion most likely has a chemical mechanism with no interference of electron transfer reactions [23-25]. However, Wu *et al.* [26,27] indicated that the organic acids could dissociate into $RCOO^-$ and H^+ in oil media at high temperature. Consequently, an electrochemical mechanism is also possible.

In the present work, the coupon morphology observed by electron microscopy showed some hints of electrochemical mechanisms. As shown in Figure 2.4, for carbon steel coupons immersed in commercial naphthenic acid in white oil (TAN = 5mg KOH/g) at AET = 300°C for 1 h, their morphological changes were those typical of general corrosion. After 4 h, corrosion pits appeared indicating that the corrosion became more selective due to a preferential attack of a particular component of the coupon. A possible explanation is that under those conditions, organic acids dissociated into $RCOO^-$ and H^+ and electrochemical corrosion mechanisms occurred.

2.4.2 The correlation between corrosivity and chemical properties of organic acids

For organic acid compounds, there were several ways in which their chemical

structures affected their corrosivity. First, molecular weight affects the diffusion coefficient of the acids. Larger organic acid molecules will have lower diffusion coefficients. Therefore, larger-sized acid molecules would reach the metal surfaces more slowly than smaller molecules and so would have lower corrosion rates. For molecules with the same molecular weight, structural features of the organic acids became important. For example the cyclohexanebutyric acid and 1-naphthoic acid have similar molecular weights. However, cyclohexanebutyric acid with a single cycloalkane ring causes significantly greater corrosion of the carbon steel coupon in the liquid than 1-naphthoic acid with two aromatic rings. The corrosion rates for carbon steel coupons immersed in the oil decrease dramatically, when R contains more than one ring. Secondly, the molecular weight of an aliphatic group or naphthenic group has an effect on the affinity of ligand $RCOO^-$ and H^+ in oil. It was suggested that the higher the molecular weight of R, the more difficulty the acid has to dissociate into $RCOO^-$ and H^+ in oil [26,27]. Therefore, the acid molecular weight will also directly affect the corrosivity of the acid. Molecules with smaller R values have a stronger capability to react with metals. Based on the above discussion, it was concluded that organic acids with higher average molecular weight would have lower corrosivity. This is consistent with the corrosion test results shown herein.

2.5 Summary

In the present study, a corrosion unit has been developed to simulate corrosion found in refinery vacuum distillation towers. Model oil mixtures were prepared using individual organic acid compounds dissolved in white oil where the organic acid compounds contained various carbon and ring numbers. Model oil mixtures in white oil were also prepared using a commercial naphthenic acid mixture.

For the commercial naphthenic acid in white oil, the corrosion rates for carbon steel coupons suspended in the condensate where acid vapors can condense increased with increasing TAN value and temperature where as the corrosion rates for the coupons immersed in the oil liquid increased with TAN value only. These results were expected as they reflect increases in acid concentration either in condensate or in the oil

liquid [15].

When individual organic acid compounds in white oil were tested for corrosivity, several conclusions were made. For corrosion of carbon steel coupons suspended in the condensate, the boiling point of the organic acid was a threshold temperature for corrosion. If the AET was below the boiling point, there was little corrosion; if the AET is above the boiling point, the lowest molecular weight, straight chain carboxylic acid was the most corrosive. For carbon steel coupons immersed in the oil liquid, the corrosion rates decreased with increasing molecular weight of the organic acid. The corrosion rates in the liquid were lower than those obtained in the condensate when AET was above the organic acid boiling point and were comparable to those found in the condensate when AET was lower than the boiling point.

2.6 References

[1] R. L. Piehl, Corrosion 1987, NACE Paper No. 196, (1987)..

[2] W.A. Derungs, Corrosion, Vol. 12, p. 41, (1956)

[3] R.L. Peihl, Vol. 27, No. 1, p. 37, (1988)

[4] J. Gutzeit, Materials Performance, Vol. 16, No. 10, p. 24, (1977)

[5] R.D. Kane, E. Trillo and J.G. Maldonaldo, In: Proceedings of Eurocrr 2003, 28 September 2003, Budapest, Hungary, (2003)

[6] H. Lee Craig, Jr., Corrosion 1996, NACE Paper No. 603, (1996)

[7] B. Messer, B. Tarleton, M. Beaton, and T. Phillips, Corrosion 2004, NACE Paper No. 04634, (2004)

[8] A. Groysman, Corrosion 2005, NACE Paper No. 05568, (2005)

[9] A. Turnbull, E. Slavcheva and B. Shone, Corrosion, Vol. 54, No. 11, p. 922. (1998).

[10] G.C. Laredo, C.R. Lopez, R.E. Alvarez and J.L. Cano, Fuel, Vol. 83, No.11, p. 1689, (2004)

[11] B. Messer, B. Tarleton, M. Beaton, T. Phillips, Corrosion 2004, NACE Paper No. 04634, (2004)

[12] B.F. Qi, X. Fei, S.J. Wang and L.R. Chen, Pet. Sci. Technol. Vol. 22, No.3–4, p. 463, (2004)

[13] M.P. Barrow, L.A. McDonnell, X.D. Feng, J. Walker and P.J. Derrick, Anal. Chem. Vol.75, No. 4, p. 860, (2003)

[14] Y. Cao and H. Shen, Corrosion Science and Protection Technology, Vol. 19, Nov. 1, p. 48, (2007)

[15] H. Mediaas, K.V. Grande, B.M. Hustad, A. Rasch, H.G. Rueslåtten, J.E. Vindstad, Society of Petroleum Engineers, paper 80404, (2003)

[16] L.I. Freiman, Protection of Metals (English translation of Zaschita Metallov), Vol. 22, No. 2, p. 149, (1986)

[17] S. Japanwala, K.H. Chung, H.D. Dettman, and M.R. Gray, Energy & Fuels, Vol. 16, p. 477, (2002)

[18] S.A. Jenabali Jahromi, A. Janghorban, Engineering Failure Analysis, Vol. 12, No. 4, p. 569, (2005)

[19] X.Q. Wu, H.M. Jing, Y.G. Zheng, Z.M. Yao and W. Ke, Corrosion Science, Vol. 46, No. 4, p. 1013, (2004)

[20] D.R. Qu, Corrosion Science Vol. 48, No. 8, p. 1960, (2006)

[22] C.J. Ballhausen., J. Chem. Educ. Vol. 56, No. 4, p. 357, (1979)

[23] H.A.*Cataldi*, R.J. Askevold and A.E. Harnsberger, Petroleum Refiner, Vol. 32, No. 7, p. 145, (1953)

[24] E. Slavcheva, B. Shone and A. Turnbull, Br.Corrosion. J, Vol. 34, No. 2, p. 125, (1999)

[25] S. Tebbal, Corrosion 1999, NACE Paper No. 380, (1999)

[26] X.Q. Wu, H.M. Jing, Y.G. Zheng, Z.M. Yao and W. Ke, Wear, Vol. 256, No. 1–2, p. 133, (2004)

[27] X.Q. Wu, H.M. Jing, Y.G. Zheng, Z.M. Yao and W. Ke, Mater. Corros. Vol. 53 No. 11-12, p. 833, (2002)

Chapter 3. Thermal Stability of Sulfur Compounds

3.1 Introduction

High temperature corrosion due to sulfur compounds normally accompanies organic acid corrosion in refinery applications [1, 2]. Sulfur occurs in crude petroleum at various concentrations, and consists of a variety of chemical compounds, including hydrogen sulfide, mercaptans, sulfides, polysulfides, thiophenes and elemental sulfur [3]. These days, the sulfur content in crude oils varies from 0.2 to 2.5 wt % on average, and it can be as high as 6 wt % in some crude oils [4].

Hydrogen sulfide is the most corrosive sulfur compound [5, 6], consequently high temperature sulfide corrosion can be divided into two steps, thermal cracking of the sulfur compounds to generate H_2S and reaction of H_2S and iron to form iron sulfide scales. Corrosion rates have been found to be dependent upon temperature, sulfur concentration and the form in which the sulfur exists [3,4,7-10]. Corrosion engineers tend to use the total sulfur as a indicator of the corrosivity of crude oil. However, total sulfur content is a poor method for estimating the probability of the eventual presence of hydrogen sulfide.

Sulfur compounds and their decomposition should be considered in most cases of high temperature corrosion due to their range of thermal stability [11-16]. Sulfur conversion is different for different sulfur compounds over the temperature range of 200~400°C because of the different carbon-sulfur bonds [17-19]. In petroleum chemistry, the thermal stability of sulfur compounds under refinery conditions has not been extensively described in the literature.

The aim of this Chapter is to determine the thermal stability of different types of carbon-sulfur bonds in order to understand the range of H_2S formation possible from petroleum during refinery thermal conditions and residence times. A series of thermal cracking experiments for specific model sulfur compounds dissolved in white oil were run and their products analysed.

3.2 Experimental Procedures

3.2.1 Sulfur compounds and test media

The nine sulfur compounds chosen for this study are shown in Table 3.1. These compounds were purchased from Sigma Chemical Company (3050 Spruce street, St. Louis, MO 63103). The test samples were prepared by mixing model sulfur compound with the white oil from Acatris Inc (2770 Portland Drive, Oakville, Ontario L6H6R4). The test mixtures were prepared to have a total sulfur content approximately 0.5 wt %. The four model sulfur compounds, diphenyl sulfide, benzyl phenyl sulfide, dodecyl sulfide and octyl sulfide were chosen to test at three temperatures (200°C, 300°C, 400°C) for 1 to 48 h, where as the remaining five model compounds were only tested at 300°C for 2 h.

Table 3.1 Model Sulfur Compounds Used in Thermal Cracking Experiments

Name	MW	Structure
Octyl sulfide	258.51	$CH_3(CH_2)_6CH_2SCH_2(CH_2)_6CH_3$
Dodecyl sulfide	370.72	$CH_3(CH_2)_{10}CH_2SCH_2(CH_2)_{10}CH_3$
Diphenyl sulfide	186.27	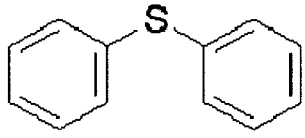
Benzyl phenyl sulfide	200.30	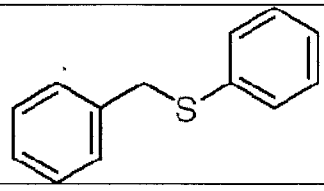
Benzyl sulfide	214.33	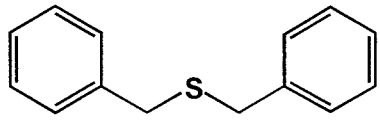
Dicyclohexyl disulfide	230.43	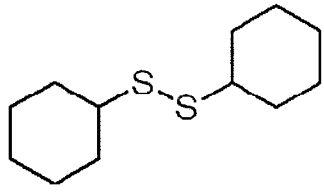
1,3-Dithiane	120.24	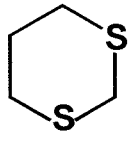
Dibenzothiophene	184.26	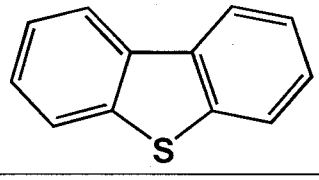
Sec-Butyl disulfide	178.36	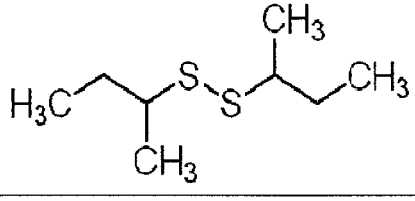

3.2.2 Autoclave unit description

The cracking experiments were conducted in a 316 stainless steel 1L stirred autoclave, shown in Figure 3.1. The vessel was charged with 300 mL test sample and sealed. It was flushed with nitrogen 3 times at 200 psi (1379 kPa) and then pressure-tested at 1500 psi (10342 kPa) for 1 h. The pressure was adjusted to approximately 220 psi (1517 kPa) and the vent valve closed. The autoclave was heated to reaction temperature and stirred at approximately 500 rpm. The inside temperature and pressure were continuously recorded at 5-s intervals and stored in Excel compatible format (CSV). At the end of the heating period, the autoclave was allowed to cool to room temperature, and then the gas was vented into a gasbag which was analyzed by gas chromatography analysis using standard refinery gas analysis procedures [22]. The oil remaining in the autoclave was drained through the bottom port into a sample collection receiver. The autoclave was then washed with toluene.Toluene was removed from the washings by evaporation in a fumehood overnight. The weights of original sample, liquid products and washings were recorded, and all liquid products were collected and sent for analysis. Examples of experimental conditions and product yields are shown in Table 3.2.

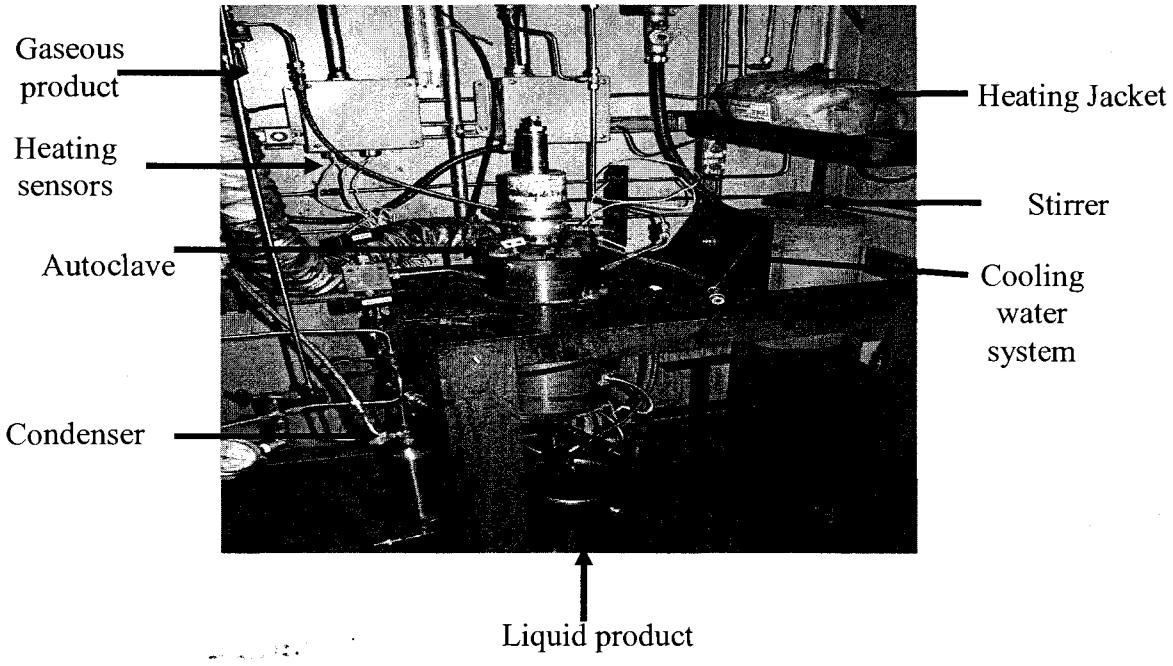

Figure 3.1 Autoclave System for Thermolysis Experiment

Table 3.2 Feed, Yield and Conditions for Thermolysis Experiments

No	Sulfur Compounds	Temp.	Time	Initial S%	Final S %	Mass balance %
1	Diphenyl sulfide	400°C	1	0.59	0.5259	99
2	Diphenyl sulfide		2	0.5	0.3998	99
3	Diphenyl sulfide		8	0.4997	0.2784	99
4	Diphenyl sulfide		16	0.5127	0.2289	99
5	Diphenyl sulfide		20	0.5452	0.2213	99
6	Diphenyl sulfide		48	0.5286	0.2126	99
7	Benzyl phenyl sulfide	400°C	1	0.5023	0.3733	98
8	Benzyl phenyl sulfide		2	0.4987	0.3561	99
9	Benzyl phenyl sulfide		4	0.5058	0.3133	99
10	Benzyl phenyl sulfide		8	0.4896	0.2905	99
11	Benzyl phenyl sulfide		16	0.5102	0.233	99

Table 3.2 continued

No	Sulfur Compounds	Temp.	Time	Initial S%	Final S %	Mass balance %
12	Benzyl phenyl sulfide		48	0.5106	0.2145	99
13	Dodecyl sulfide	400°C	1	0.5335	0.2876	98
14	Dodecyl sulfide		2	0.5356	0.2644	97
15	Dodecyl sulfide		4	0.5354	0.2256	97
16	Dodecyl sulfide		8	0.5276	0.2107	97
16	Dodecyl sulfide		20	0.5048	0.2056	98
17	Dodecyl sulfide		48	0.5048	0.2056	98
18	Octyl sulfide	400°C	1	0.5074	0.2435	98
19	Octyl sulfide		2	0.5473	0.1791	97
20	Octyl sulfide		4	0.4926	0.1605	98
20	Octyl sulfide		20	0.5132	0.1642	97
21	Octyl sulfide		48	0.5132	0.1642	97
22	Diphenyl sulfide	300°C	1	0.5121	0.5038	99
23	Diphenyl sulfide		2	0.4992	0.4906	99
24	Diphenyl sulfide		4	0.5213	0.4879	99
25	Diphenyl sulfide		20	0.5207	0.3749	99
26	Diphenyl sulfide		48	0.5211	0.2457	99
27	Benzyl phenyl sulfide	300°C	1	0.5103	0.4915	99
28	Benzyl phenyl sulfide		2	0.521	0.4521	99
29	Benzyl phenyl sulfide		4	0.542	0.4255	99
30	Benzyl phenyl sulfide		16	0.5142	0.3403	98
31	Benzyl phenyl sulfide		48	0.5209	0.2799	98
32	Dodecyl sulfide	300°C	1	0.5312	0.3645	98
33	Dodecyl sulfide		2	0.521	0.2743	97
34	Dodecyl sulfide		4	0.5345	0.2287	97
35	Dodecyl sulfide		48	0.521	0.2223	97
36	Octyl sulfide	300°C	1	0.5413	0.4425	98
37	Octyl sulfide		2	0.53765	0.3146	98
38	Octyl sulfide		4	0.5401	0.3145	99
39	Octyl sulfide		20	0.5108	0.2046	98
40	Diphenyl sulfide	200°C	1	0.5177	0.517	99
41	Diphenyl sulfide		2	0.529	0.5289	99
42	Diphenyl sulfide		16	0.5197	0.5128	99
43	Diphenyl sulfide		48	0.5225	0.5089	99

Table 3.2 continued

No	Sulfur Compounds	Temp.	Time	Initial S%	Final S %	Mass balance %
44	Benzyl phenyl sulfide	200°C	1	0.5097	0.4921	99
45	Benzyl phenyl sulfide		2	0.5487	0.4961	99
46	Benzyl phenyl sulfide		16	0.5018	0.3833	99
47	Benzyl phenyl sulfide		48	0.5327	0.3185	99
48	Dodecyl sulfide	200°C	1	0.5436	0.4553	99
49	Dodecyl sulfide		2	0.5247	0.3944	98
50	Dodecyl sulfide		8	0.5214	0.3256	98
51	Dodecyl sulfide		20	0.5612	0.2807	98
52	Octyl sulfide	200°C	1	0.5003	0.4547	99
53	Octyl sulfide		2	0.5169	0.3717	99
54	Octyl sulfide		8	0.4996	0.2674	99
55	Octyl sulfide		20	0.5132	0.2537	98

2.2.3 Analytical methods

Elemental CHN (Carbon, Hydrogen, Nitrogen) analyses were determined using ASTMD5291 on a LECO CHN-1000 Analyzer.

Gas chromatography fitted with a sulfur chemiluminescence detector (GC-SCD) was used for sulfur determination in feed and products. The GC was a Hewlett Packard gas chromatograph HP6890 series, equipped with SCD front detector (SIEVERS 355). The total sulfur contents, as shown in Table 3.2, were calculated by using the factors determined from running the sulfur standards with known sulfur concentrations. Sulfur speciation for the feeds and products was achieved by comparing GC-SCD plots of the test samples with those of sulfur standards.

3.3 Results

3.3.1 Analysis of sulfur fractions

Sulfur in gas products

Figure 3.2 shows the GC-SCD plot of the gas product resulting from the thermal cracking of octyl sulfide at 300°C and a 2 h residence time. In the gas product from octyl sulfide, the major form of sulfur was H_2S (Figure 3.3). The gas products for all other sulfur compounds tested were similar except having different quantities of H_2S. The H_2S yields in gas with time and temperature were calculated and plotted in Figure 3.3.

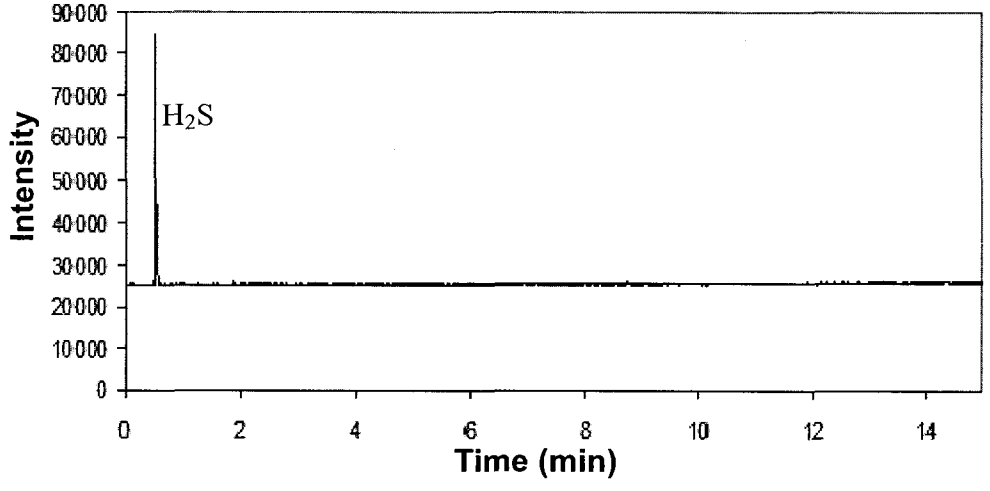

Figure 3.2 GC-SCD Plot of Gas Product Resulting from Thermolysis of Octyl Sulfide in White Oil at 300°C for 2 h

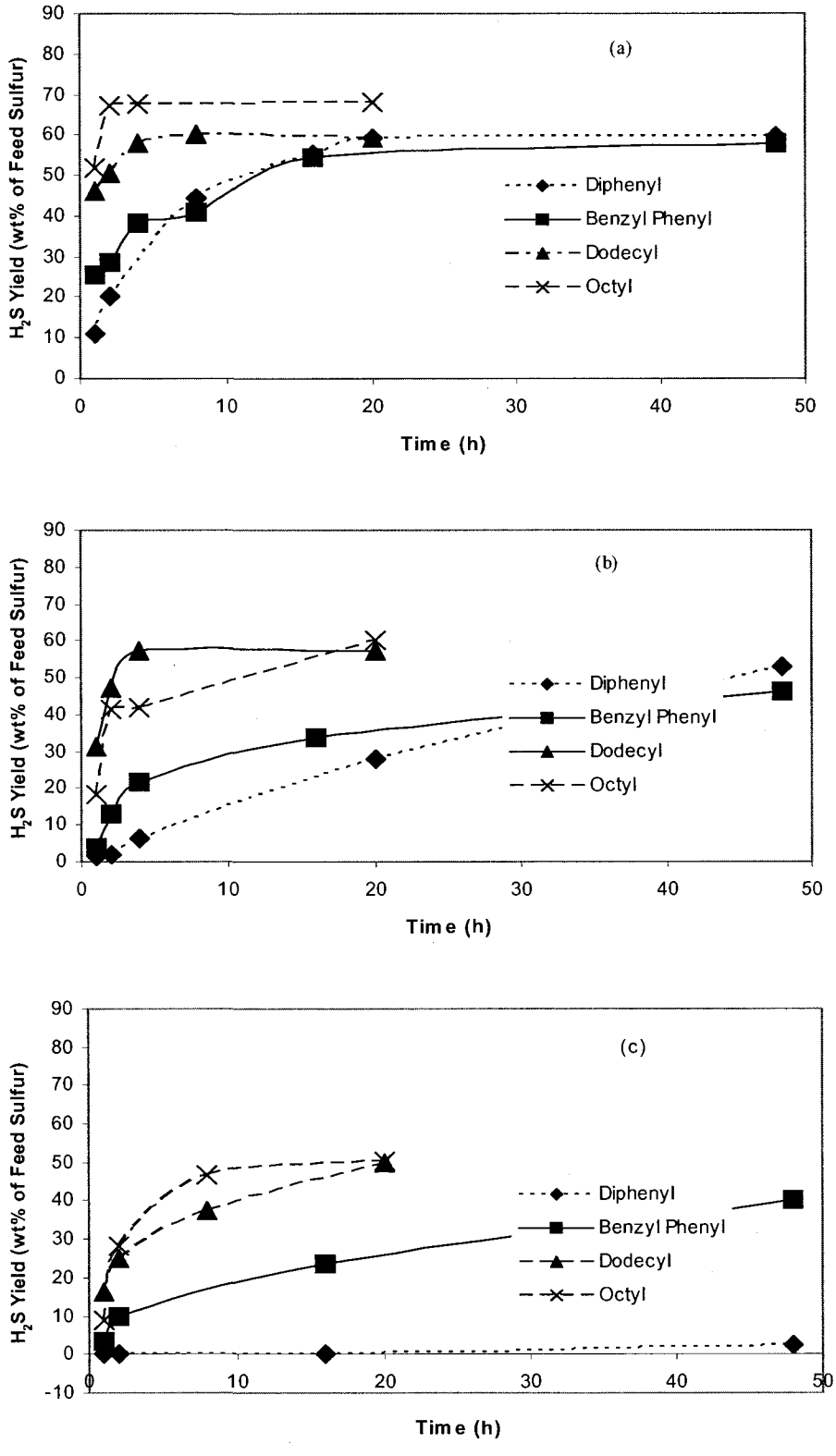

Figure 3.3 H_2S Yield in Gas from Thermolysis of Different Sulfur Compounds in White Oil with Time at (a) 400 °C, (b) 300 °C, and (c) 200 °C

Under most conditions, the order of the yield of H_2S gas generated by cracking was: octyl sulfide, dodecyl sulfide, benzyl phenyl sulfide, and diphenyl sulfide as showed in Figure 3.3(a) and (c). In Figure 3.3 (b), the H_2S yield has the same order except that dodecyl sulfide generated more H_2S gas than octyl sulfide from 2 h to 16 h.

Generally, the H_2S yield increased with temperature and time. At higher temperature (400°C), all four compounds generated H_2S during the runs. The H_2S yield of octyl sulfide and dodecyl sulfide increased more rapidly during residence times of 1 to 4 h, than that of diphenyl sulfide and benzyl phenyl sulfide. At the lowest temperature (200°C), approximately half of the octyl sulfide and dodecyl sulfide convert to H_2S, where as little H_2S was formed under these conditions with diphenyl sulfide.

Sulfur in liquid products

The sulfur species in liquid were also identified by GC-SCD analysis. Most the H_2S generated during thermal conditions was found in the gas product. However there was always a small quantity of H_2S dissolved in the liquid product (Figure 3.4). Figures 3.5-3.8 show the GC-SCD results of the different sulfur species generated during thermolysis of the four sulfur compounds at 300°C for 2 h.

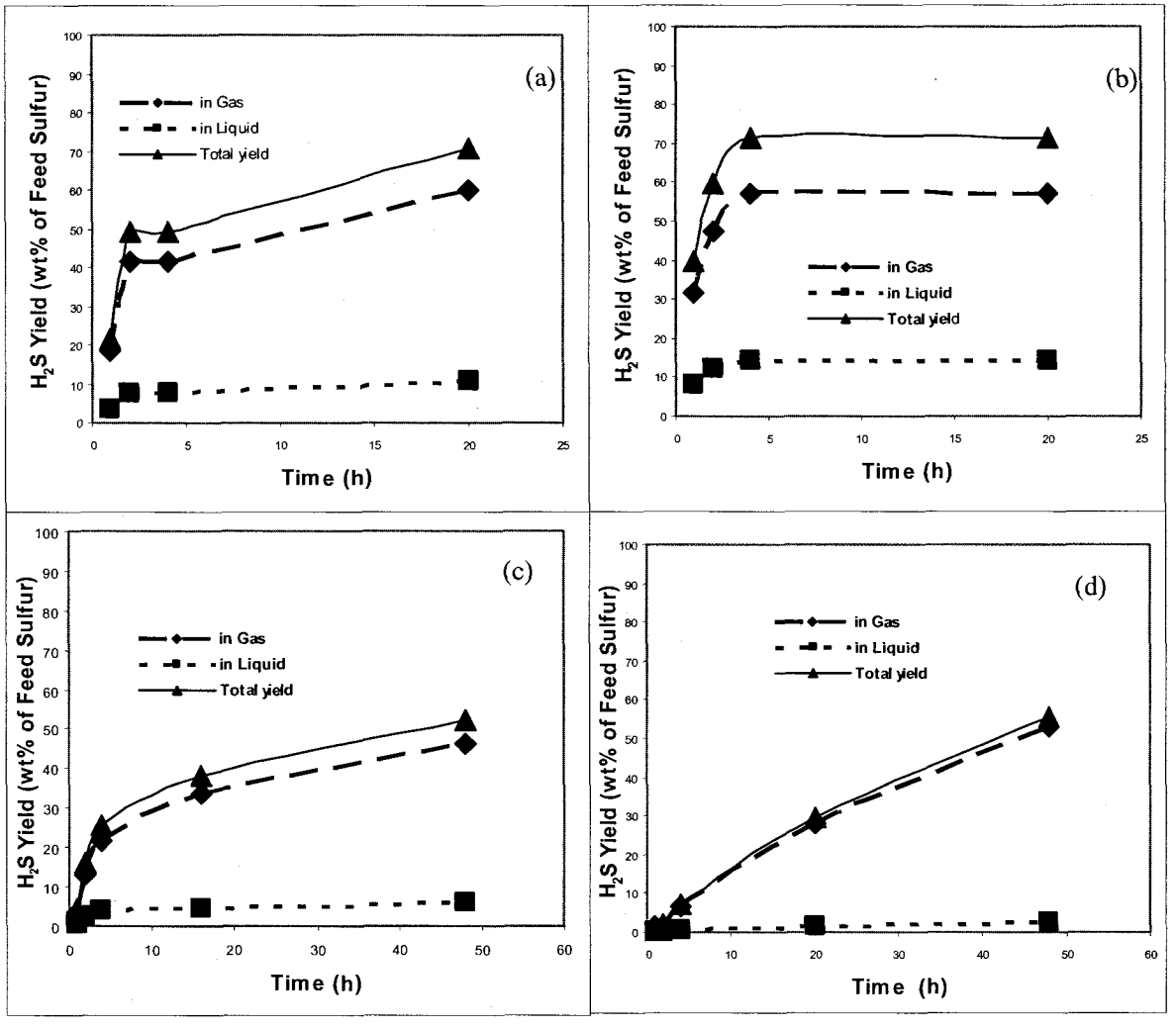

Figure 3.4 H_2S Yield from Thermolysis of Different Sulfur Compounds in White Oil at 400°C (a) Octyl Sulfide, (b) Dodecyl Sulfide, (c) Benzyl Phenyl Sulfide, and (d) Diphenyl Sulfide

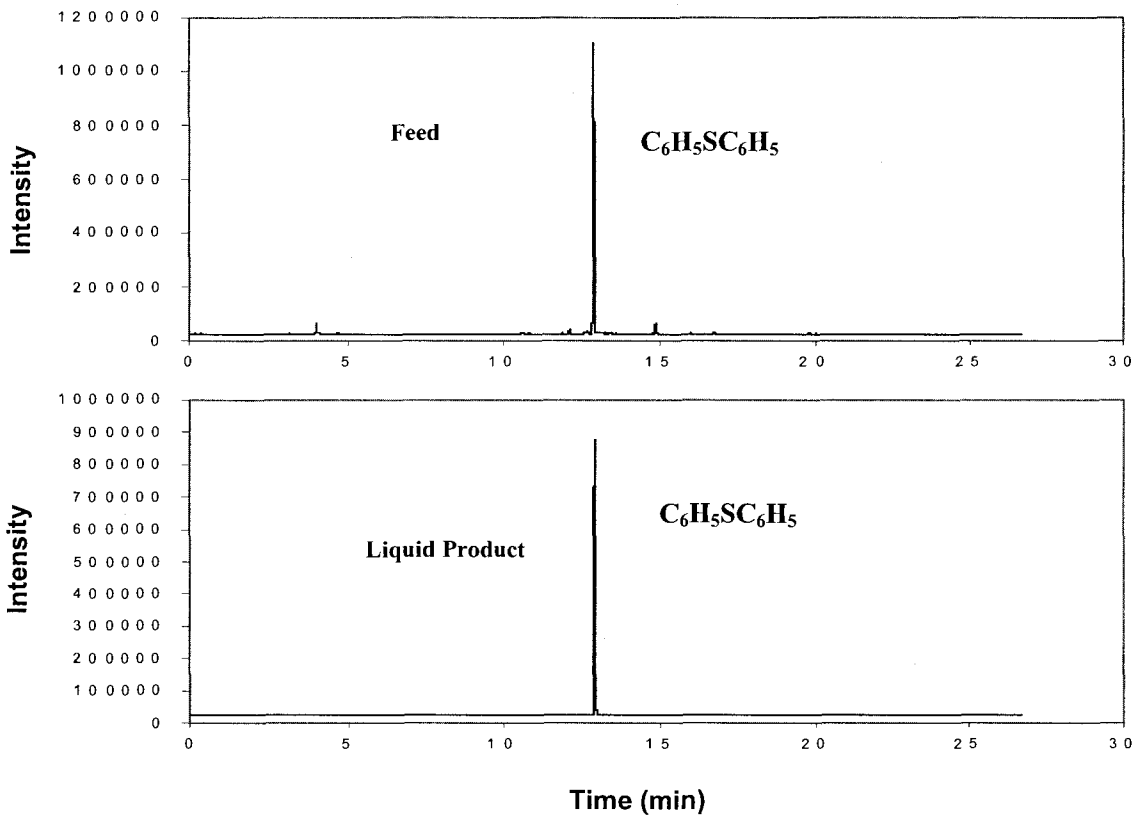

Figure 3.5 GC-SCD Plots of Feed and Liquid Product Resulting from Thermolysis of Phenyl Sulfide in White Oil at 300°C for 2 h

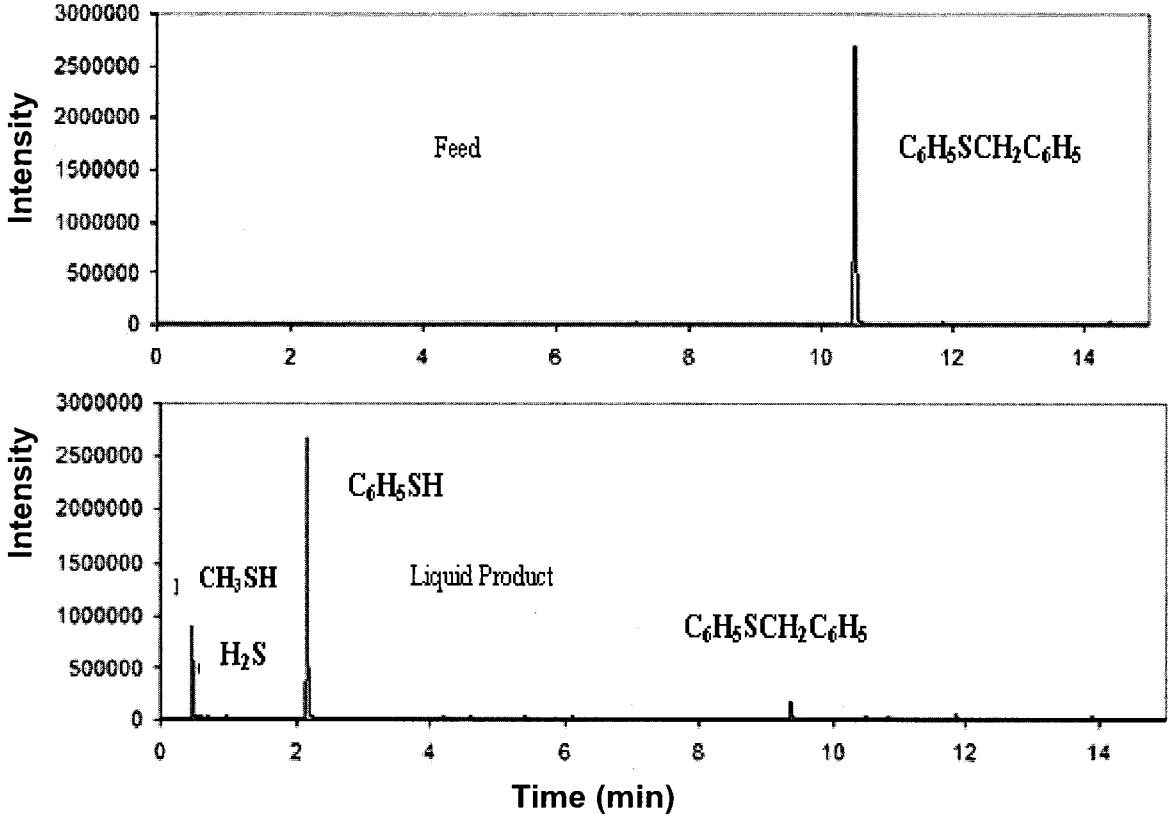

Figure 3.6 GC-SCD Plots of Feed and Liquid Product Resulting from Thermolysis of Benzyl Phenyl Sulfide in White Oil at 300°C for 2 h

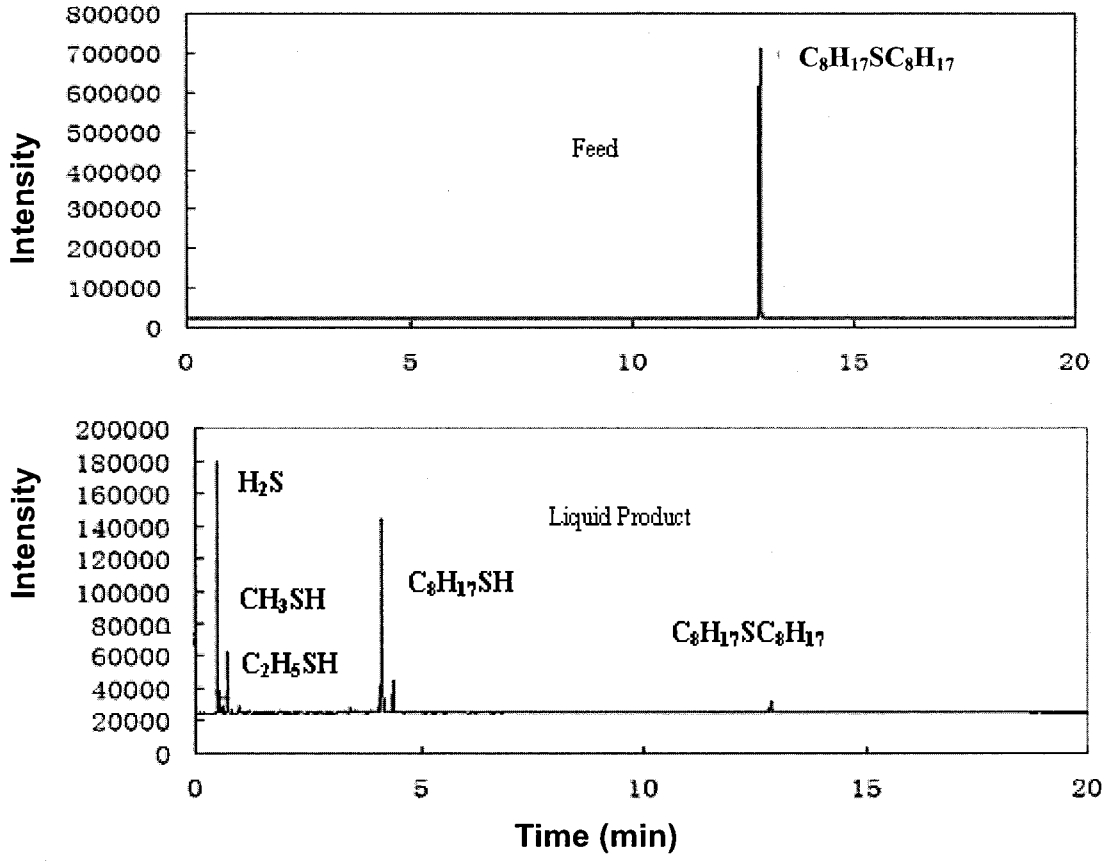

Figure 3.7 GC-SCD Plots of Feed and Liquid Product Resulting from Thermolysis of Octyl Sulfide in White Oil at 300°C for 2 h

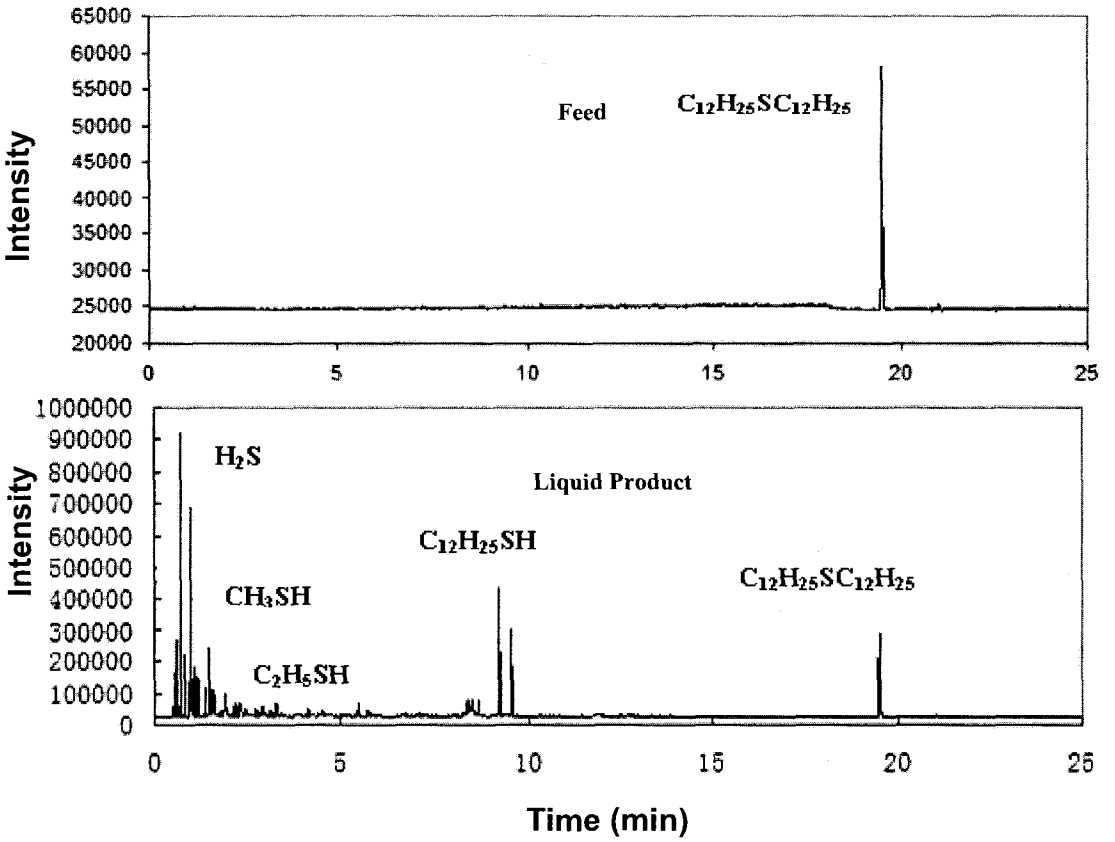

Figure 3.8 GC-SCD Plots of Feed and Liquid Product Resulting from Thermolysis of Dodecyl Sulfide in White Oil at 300°C for 2 h

The plots in Figures 3.5 to 3.8 show that methyl mercaptan and ethyl mercaptan were formed in most of the liquid products, particularly during conversion of octyl and dodecyl sulfides. This demonstrates that as the sulfur was removed from the compounds, it was able to combine with small radicals other than hydrogen generated during the thermal cracking of the white oil. Other sulfur-containing products generated included mercaptans formed by cleavage of only one side of the C-S-C bond. For example, a major sulfur-containing product of the thermolysis of benzyl phenyl sulfide, was phenyl mercaptan. This indicates the C-S bond on the methylene side was the easier bond to break.

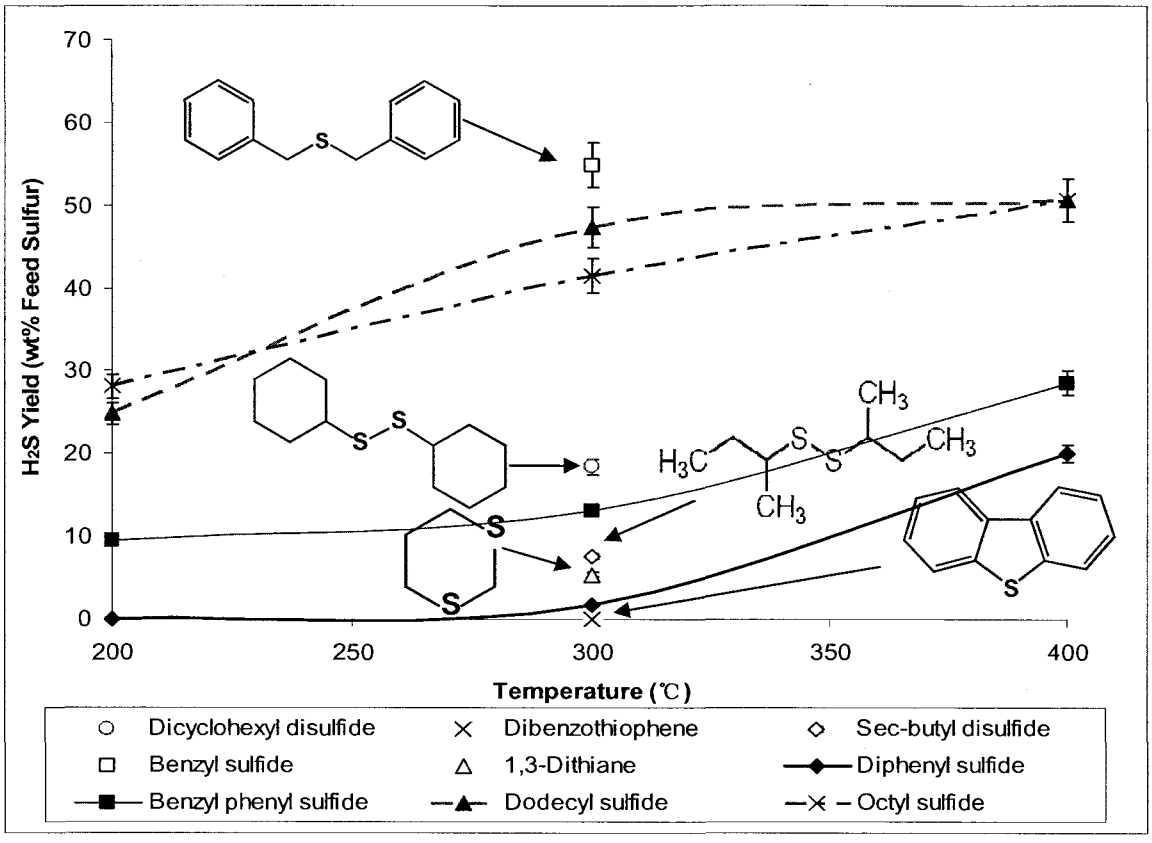

Figure 3.9 H_2S Yield from Thermolysis of Different Sulfur Compounds in White Oil at 300°C for 2 h

Sulfur conversion was also measured for the thermolysis of five other sulfur compounds at 300°C for 2 h. As Figure 3.9 shows, different molecular structures determine different thermal stabilities and result in significant differences in yields of H_2S. Under the specified conditions, dibenzothiophene was the most stable, where no H_2S was observed. In contrast, benzyl sulfide was most active where more than half of the sulfur was converted into H_2S gas. The results show that the C-S bonds in ring structures are more stable than those in chains. For example, there is less H_2S generated by 1,3-dithiane or dibenzothiophene than octyl sulfide or benzyl sulfide. Upon comparing two disulfides, dicyclohexyl disulfide and sec-butyl disulfide, the sulfur attached to the cyclohexane ring methyne carbon was more stable than the sulfur

attached to the chain methyne carbon.

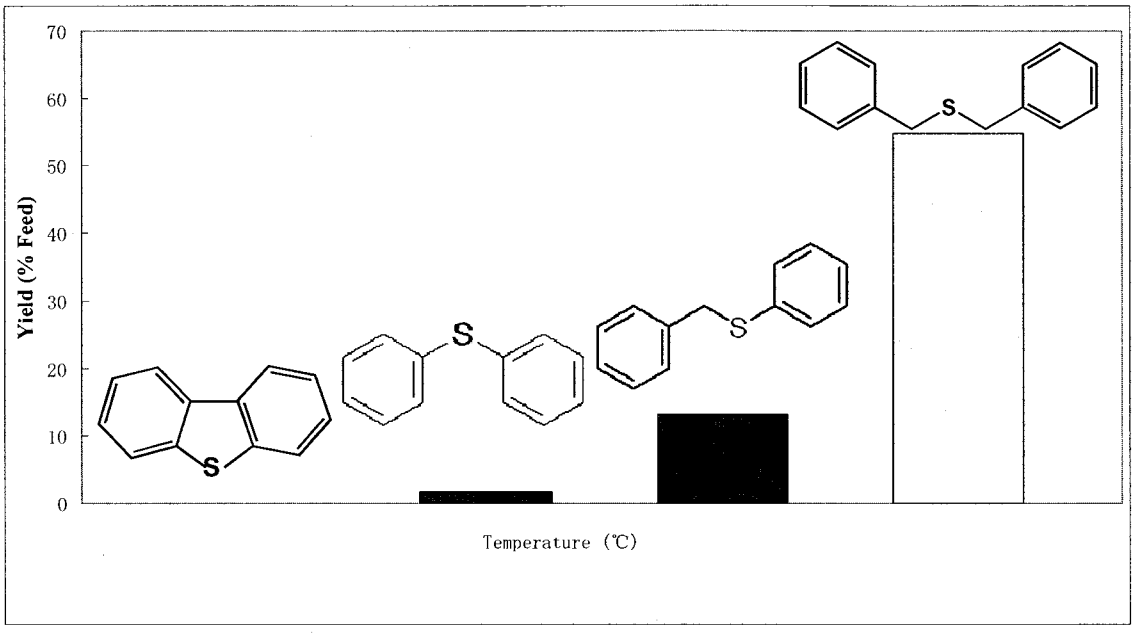

Figure 3.10 H_2S Yields from Thermolysis of Compounds with Similar Structures in White Oil at 300°C for 2 h

Figure 3.10 shows the formation of hydrogen sulfide during thermal treatment of three similar sulfur compounds, diphenyl sulfide, benzyl phenyl sulfide and benzyl sulfide. After 2 h at 300°C, little H_2S has evolved from dibenzothiophene where as the greatest quantity evolved from benzyl sulfide.

3.3.2 Kinetics of sulfur thermal cracking

The activation energies have been calculated, using the sulfur conversion data of four model sulfur compounds, diphenyl sulfide, benzyl phenyl sulfide, dodecyl sulfide and octyl sulfide. Using the total sulfur content in liquid shown in Table 3.2, the equation for the sulfur removal for all thermal processes can be expressed as [20,21]

$$-\frac{dC}{dt} = kC^n \qquad (3.1)$$

The integrated form of Equation (3.1) is

$$C^{1-n} - C_0^{1-n} = (n-1)kt \quad n \neq 1 \qquad (3.2)$$

where C is the sulfur concentration at reaction time t, C_0 is the initial sulfur concentration, k is the apparent rate constant for sulfur removal from sulfur species lumped together, and n is the apparent reaction order.

The results for diphenyl sulfide are used as an example for calculation of the kinetic order. The sulfur concentration and liquid yields obtained in the runs are indicated in Table 3.2. The data from Table 3.2 were tested for different kinetic orders in Equation (3.2), and the fit was determined by linear regression (Figure 3.11). The best fit for diphenyl sulfide thermal cracking corresponded to n = 1.1 and is shown in Figure 3.11.

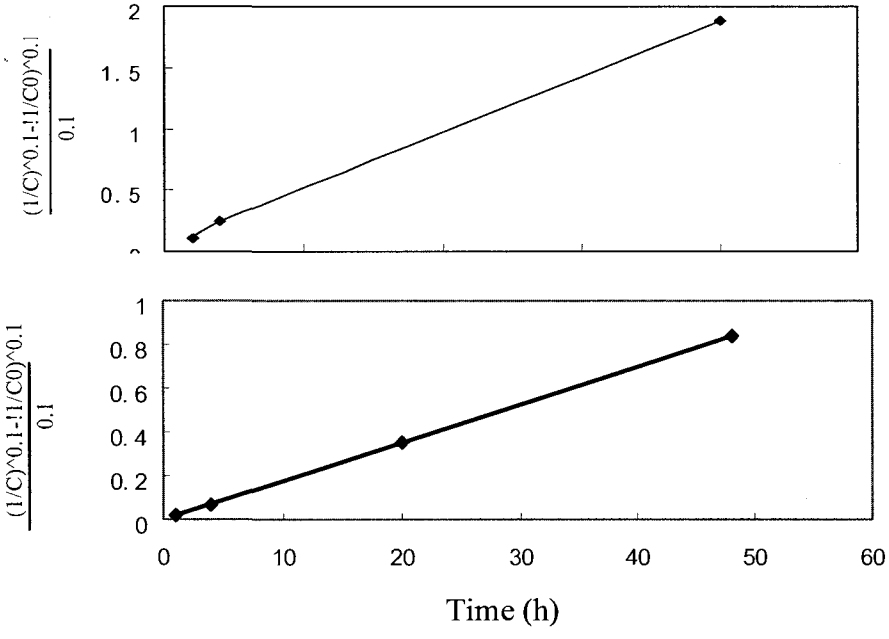

Figure 3.11 1.1th Order Kinetic Plot for Thermal Cracking of Diphenyl Sulfide

The 1.1-order rate equation is given by

$$\frac{(1/C)^{0.1} - (1/C_0)^{0.1}}{0.1} = kt \qquad (3.3)$$

The temperature dependence of the reaction-rate constants obtained was assumed to follow the Arrhenius equation,

$$k=A*\exp^{(-Ea/R*T)} \qquad (3.4)$$

where A is pre-exponential factor. The plot of ln[k] versus 1/T gives a linear plot with a negative slope where Ea is the activation energy for the reaction in kJ/mole, R is the ideal gas law constant (8.314 J/mole K), and temperature (T) is measured in Kelvin.

Solving for two different temperatures T_1 and T_2, we can obtain the following equation:

$$\ln\left(\frac{k_1}{k_2}\right) = \frac{E_a}{R}\left(\frac{1}{T_2} - \frac{1}{T_1}\right) \qquad (3.5)$$

where k is calculated by Equation (3.3). The plot of ln(k) versus 1/T (Arrhenius Plot) results is a straight line where the slope gives the activation energy (Figure 3.12).

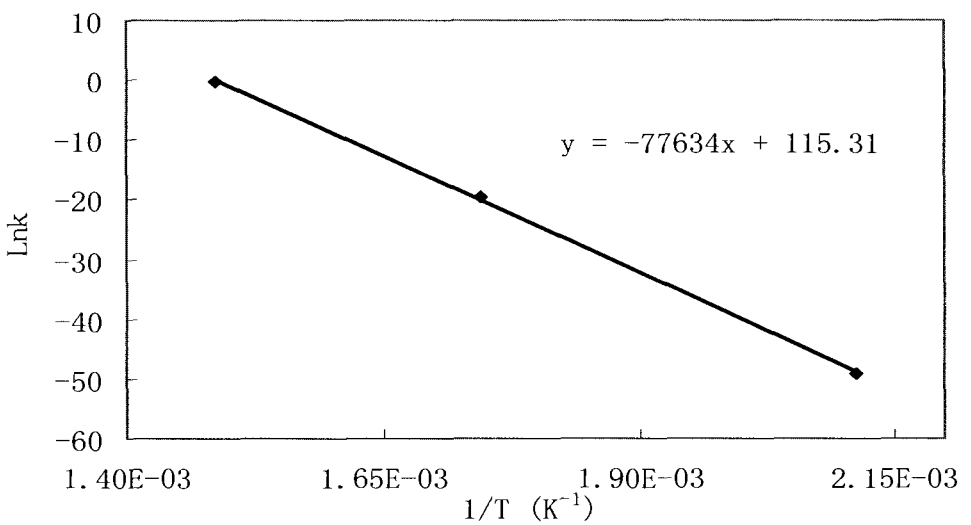

Figure 3.12 Arrhenius Plot of Diphenyl Sulfide

The kinetic orders and activation energies of the other three compounds were calculated the same way and the results are listed in Table 3.3.

Table 3.3 Kinetic Orders and Activation Energies for Thermal Conversion of Sulfur Compounds

Model Compound	Kinetic order	E_a (kJ/mol)
Diphenyl sulfide	1.1	645
Benzyl phenyl sulfide	1.2	233
Octyl sulfide	1.3	126
Dodecyl sulfide	1.3	122

From Table 3.3, the activation energy for thermal cracking of diphenyl sulfide is 645 kJ/mol and is much higher than those of the other three compounds. This indicates that diphenyl sulfide is the most stable of the four model compounds. The least stable C-S bonds were found in octyl sulfide and dodecyl sulfide, where as the benzyl phenyl sulfide had an activation energy between the two extremes. Taken all together, these results show that sulfur bonded to methylene groups are less thermally stable than sulfur bonded to quaternary aromatic carbon.

3.4 Discussion

In hydrocarbons and sulfur compounds with similar structures, the activation energies of C-S bonds are lower than those of the C-C bonds [22-25]. Thermolysis studies have shown that the typical range of activation energies for aliphatic C-C bonds is from 200-350 kJ/mol [24-26], where as that of an alkyl C-S bond has been reported to be 270 kJ/mol [26]. However there is little information in the literature on the ranges of activation energies for C-S bonds.

Table 3.3 shows that the activation energies of C-S bonds ranged from 122 to 646 kJ/mol. Comparison of these results to those in Figure 3.9 shows that the dibenzothiophene is more stable than diphenyl sulfide. This suggests that the

dibenzylthiophene C-S bonds have activation enerygies higher than the 646 kJ/mol measured for diphenyl sulfide. The least stable compound tested was benzyl sulfide. Consequently the activation energies for the C-S in benzyl sulfide are slightly lower than the 122 kJ/mol measured for octyl sulfide. Figure 3.9 also shows that the relative sulfur conversion of two disulfides, dicyclohexyl disulfide and sec-butyl disulfide. The activation energies of these species would appear to be in the range of 200 to 600 kJ/mol. This result for disulfides is interesting as disulfides are expected to have relatively low activation energies. For example the S-S bond in benzyl disulfide was reported to be 230 kJ/mol [29]. It can be explained that during thermolysis, the S-S bonds are most easily cracked so that the formation of H_2S depends upon rate of cleavage of the C-S bonds. However this needs to be confirmed.

From the results of the kinetic calculation (Table 3.3), the highest to lowest activation energies of the C-S bonds were diphenyl sulfide, benzyl phenyl sulfide, dodecyl sulfide and octyl sulfide (Figure 3.5~3.8). The strength of the diphenyl sulfide C-S bonds suggests that the C-S bond becomes stabilized by the aromatic ring. This is supported by the benzyl phenyl sulfide results, where the benzyl C-S bond is the most labile bond and phenyl mercaptan is left as an intermediate product. As well, the most stable C-S bonds are those in ring structures such as dibenzothiophene in Figure 3.9. Sulfur does not have lone-pair electrons so can not participate in π bonding. However, the π bonding in which its attached carbon participates appears to stabilize the C-S bond in these three examples. The 1,3-dithiane results show that sulfur attached to methylene carbon in a ring is more stable than if it is attached to methylene carbon in a chain. The rigidity of ring structure appears to give added stability to the 1,3 dithiane C-S bonds.

3.5 Summary

Nine model sulfur compounds dissolved in white oil have been thermally treated between 200 and 400°C for 1 to 48 h. All compounds except dibenzothiophene decomposed to produce gas and liquid products. H_2S was the major gas product. Sulfur species in the liquid products included unconverted model compound, dissolved H_2S and mercaptans.

Sulfur conversion was different for different sulfur compounds because of the different chemical bond structures. For example at 300°C and residence time of 2 h, the most unstable C-S bonds were in dibenzyl sulfide where over 50 wt% of feed sulfur was converted to H_2S. Under the same conditions dibenzothiophene had the most stable C-S bonds where 0 wt% H_2S was produced. Methylene C-S bonds in chains were the most thermally unstable of the compounds tested. Methylene C-S bonds in rings were more stable than those in chains. Disulfide compounds containing methyne C-S bonds were more stable than sulfur compounds containing methylene chain C-S bonds. For sulfur attached to aromatic ring carbons, C-S bonds were the most stable. Even though sulfur can not participate in π bonding because it does not have lone-pair electrons, the π bonding in which its attached carbon participates appears to stabilize the C-S bond.

3.6 References

[1] A. Jayaraman and R.C. Saxena, Corros. Prev. Control, Vol. 42, No. 6, p. 123, (1995)

[2] H. L. Craig, Corrosion 1995, NACE Paper No. 333, (1995)

[3] E. L. Garverick, Corrosion in the Petrochemical industry, ASM International, Materials Park OH, p. 204, (1995)

[4] R. A. White, Materials Selection for Refineries and Associated Facilities, National Association of Corrosion Engineers, Houston, Texas, (1991)

[5] R.L. Phiel, Corrosion, Vol. 16, p. 139, (1960)

[6] A.S. Couper, A. Dravnieks, Corrosion, Vol. 18, p. 291, (1962)

[7] Z.A.Foroulis, Anti-Corrosion Vol. 32, p. 4, (1985)

[8] J. Gutzeit, Materials Performance, Vol. 16, No. 10, p. 24, (1977)

[8] H. F. McConomy, Proceedings API, Vol. 43 (III). p. 78, (1963)

[10] J. Hucińska, Advances in Materials Science, Vol. 6, No. 1, p. 9, (2006)

[11] F. Behar, P. Ungerer, S. Kressmann and J.L.Rudkiewicz, Rev. Inst. Fr. Pit., Vol. 46, No. 2, P. 151, (1991)

[12] F.Behar, S. Kressmann, and J.L. Rudkiewicz, Organic Geochemistry, Vol. 19, P. 173, (1991)

[13] F. Behar and M. Vandenbroucke, Energy and Fuels, Vol. 10, p. 932, (1996)

[14] F. Behar, Y. Tang and M. Vandenbroucke, M., Organic Geochemistry, Vol. 26, p. 321, (1997)

[15] F. Behar and H.Budzinski, Energy and Fuels, Vol. 13, p. 471, (1999)

[16] F. Behar, F. Lorant, and H. Budzinski, Energy and Fuels, Vol. 16, p. 831, (2002)

[17] F. Behar, P. Chaverot, M. Berthelin, Industrial Engineering and Chemical Research, Vol. 27, p. 1529, (1998)

[18] R. Bounaceur, G. Scacchi, P.M. Marquaire, Industrial Engineering and Chemical Research, Vol. 39, p. 4152, (2000)

[19] F. Domine, R. Bounaceur, G. Scacchi, P.M. Marquaire, D. Dessort, B. Pradier, , O. Brevart, Organic Geochemistry, Vol. 33, p. 1487, (2002)

[20] B.M. Fabuss, J.O. Smith, C.N. Satterfield, Advances in Petroleum Chemistry and Refining, Vol. 9, p. 157, (1964)

[21] H. Freund, International Journal of Chemical Kinetics, Vol. 21, p. 561, (1989)

[22] S. D. Raseev, Thermal and Catalytic Processes in Petroleum Refining, Published by CRC Press, p. 13, (2003)

[23] M. R. Gray, Upgrading Petroleum Residues and Heavy Oils, Marcel Dekker, INC., p. 83, (1995)

[24] M. L. Poutsma, Energy Fuels, Vol. 4, p.113, (1990)

[25] F. Khorasheh and M.R.Gray, Ind. Eng. Chem. Res, Vol. 32, p1853, (1993)

[26] S. W Benson, Thermochemical Kinetics, 2nd ed.; John Wiley and Sons: New York, (1976)

[27] P. E.Savage, M. T. Klein, and S. G. Kukes, Ind. Eng. Chem. Des., Vol. 24, p.1169, (1985)

[28] P. E.Savage, M. T. Klein, and S. G. Kukes, Energy Fuels, Vol. 2, p.619, (1988)

[29] M. Bajus, V. A. Nikonov, A. Senning, G. V. Leplyanin, Sulfur reports, Vol. 9, No. 1, p.1, (1989)

Chapter 4. Influence of Sulfur Compounds on Organic Acid Corrosion

4.1 Introduction

High temperature corrosion of crude oil in refineries is quite complicated due to multiple factors as discussed in Chapters 1 and 2. Sulfur species not only can cause sulfidic corrosion [1-7] but can also influence organic acid corrosion [8-10]. However when a crude oil or its distillate fractions cause corrosion of steel, it is not possible to separate and quantify the relative contributions of the acid and sulfur species. According to corrosion reactions [Equations (1.1), (1.2) (1.3)] and the phase diagram for organic acid (RCOOH), hydrogen sulfide (H_2S) and iron (Fe) system (Figure 1.2), the sulfur compounds may: (1) inhibit, (2) assist or (3) do not affect the organic acid corrosion.

As discussed in Chapter 3, at elevated temperatures different sulfur compounds have different thermal stabilities, and so produce different quantities of H_2S that react with metal surfaces to form iron sulfides. The iron sulfides are insoluble in oil and so form a macroscopic film that is called a "pseudo-passive film" [13,14] because it can protect metal surfaces from the attack of organic acid and further sulfidic attack. Consequently, the "pseudo-passive film" has great influence on the synergy between organic acid corrosion and sulfidic corrosion.

In this chapter, a study of the influence of different types and content of sulfur compounds on the organic acid corrosion process is reported. The performance of different materials is also evaluated.

4.2 Experimental Procedures

4.2.1 Materials and media

Three kinds of materials from Caproco (4815 Eleniak Road, Edmonton, Alberta,

Canada T6B2N1), carbon steel (1018 CS) and two alloying stainless steels (410 SS and 316 SS) were selected. The chemical compositions are given in Table 4.1. All coupons were prepared using the method described in Chapter 3.

Table 4.1 Chemical Compositions of Carbon and Stainless Steels (wt%)

Materials	C	Cr	Ni	Mo	Mn	Si	P	S	Fe
1018 CS	0.14	–	–	–	0.76	0.10	0.017	0.038	Balance
410 SS	0.09	12.5	0.75	0.43	0.31	0.09	0.013	0.0026	Balance
316 SS	0.07	17.46	13.01	2	1.43	0.09	0.023	0.0015	Balance

The commercial naphthenic acid described in Chapter 2 and selected sulfur compounds described in Chapter 3 were used to study the influence of the interactions of organic acid and sulfur species on corrosion. The TAN values of the test media prepared with commercial naphthenic acid were approximately 5 mg KOH/g. Corrosion tests were conducted at 250°C under vacuum of 300 mbar to achieve AET equals to 300°C. The two sulfides, diphenyl sulfide and octyl sulfide were chosen to study the effects of sulfur. From Chapter 3, under the thermal conditions used during the corrosion tests, octyl sulfide was found to be very labile where as phenyl sulfide was relatively stable. The concentrations of the sulfides in the white oil were varied to obtain sulfur contents of 0.5 wt% to 2 wt%.

4.2.2 Corrosion test method

The corrosion apparatus and operating procedures were the same as those described in Chapter 3. Metal coupon specimens were degreased by washing with acetone, dried in air, and weighed before and after tests. After corrosion tests with the commercial naphthenic acid, there was little corrosion product deposited resulting in the coupons having matt surfaces. When sulfur compounds were introduced, black corrosion products formed a film on the coupons which were visible by naked eye. After tests, specimens were carefully rinsed with acetone to maintain the films, dried in air and observed by electron microscopy to study morphology. Finally, corrosion films were removed by washing in acetone, rinsing under running water, rinsing in distilled

water, and then dried in air and weighed. The corrosion rate was calculated as described in Chapter 3.

4.2.3 Microstructure analysis and morphology observation

A HITACHI S-2500 scanning electron microscope with INCAx-act energy dispersive x-ray spectroscopy (EDX) capability was used for morphology observation and composition analyses of coupon surfaces. Measurements were performed at room temperature using a 20 kV accelerating voltage.

4.3 Results

4.3.1 Sulfidic corrosion

Both materials, carbon steel and 410 stainless steel, were tested in two model oil mixtures at AET=300°C. The first model mixture consisted of octyl sulfide in white oil where as in the second mixture the octyl sulfide was replaced with phenyl sulfide. The sulfur contents of both mixtures were 1.0 wt%. The corrosion rates are plotted as a function of time in Figure 4.1.

For octyl sulfide, the sulfidic corrosion increased with test duration untill 8 h, and then decreased. This behavior can be attributed to the formation of an iron sulfide film that protects the metal surfaces. The growth of the film follows parabolic law [13]. The corrosion caused by phenyl sulfide was very low because this compound is relatively stable and therefore generates little H_2S under the thermal conditions used (see Chapter 2). Figure 4.1 also shows that 410 stainless steel has much higher sulfidic corrosion resistance than carbon steel in both sulfur compounds.

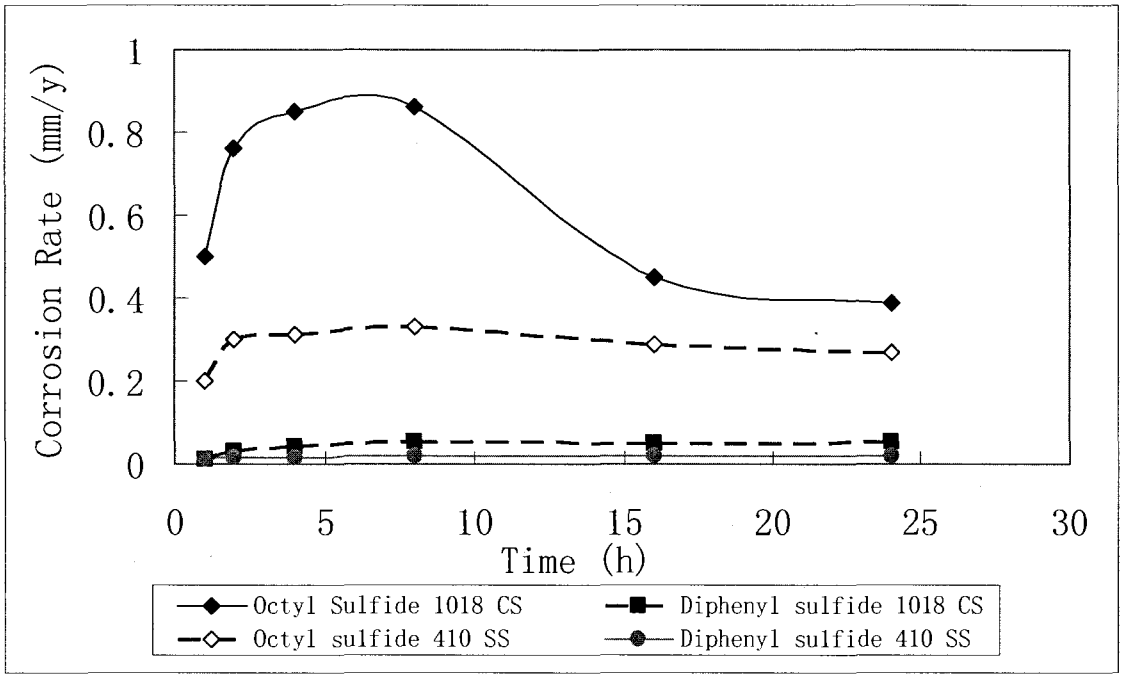

Figure 4.1 Corrosion Rates of Carbon Steel (1018 CS) and 410 Stainless Steel (410 SS) Coupons in Liquid of Model Oil Mixtures with Time (Sulfur Content = 1 wt%, AET = 300°C)

The electron micrographs showing the surface morphologies of the coupons after sulfidic corrosion are given in Figure 4.2. After corrosion, the black iron sulfide deposits can be observed especially on the surface of the carbon steel coupons. The sulfide deposits increased with time for both materials. For carbon steel, the deposits became wide and began to connect with each other by 4 h [Figure 4.2(d)]. By 48 h, the deposits had formed a continuous film [Figure 4.2(f)]. For 410 stainless steel, there were lower quantities of iron sulfide deposits formed at all test durations. An important difference from the carbon steel coupons was that white speckles appeared on the surface of 410 stainless steel. Those speckles were dispersed over the surface of the coupon by the 48 h test [Figure 4.2(e)]. EDX analyses (Table 4.2) show that the white speckles [i.e. area A in Figure 4.2 (e)] were rich in chromium, and depleted in iron and sulfur compared to an area B without white speckles [i.e. area B in Figure 4.2 (e)]. This indicates that the Cr increases the metal resistance to sulfidic corrosion.

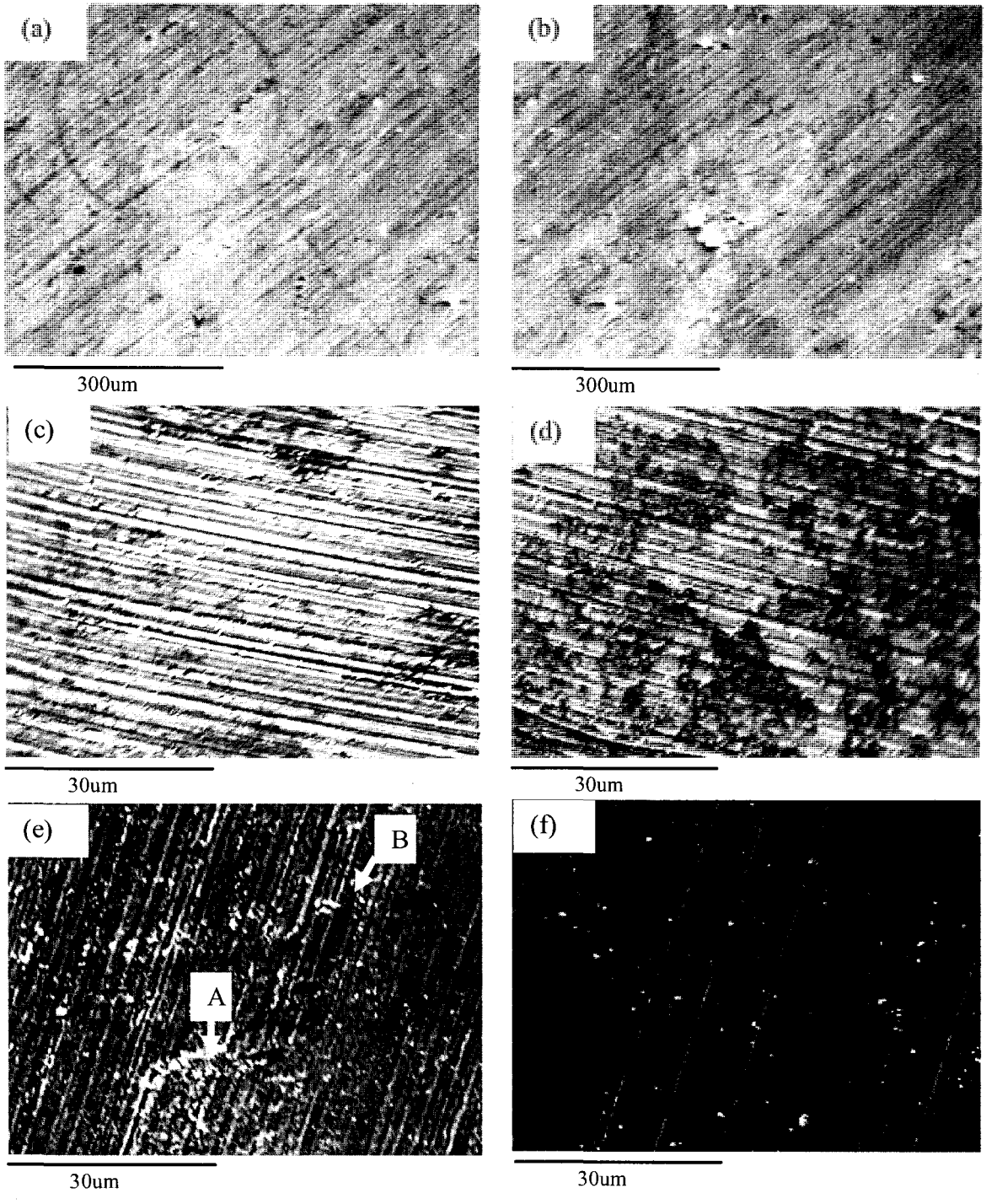

Figure 4.2 Electron Micrographs of Carbon Steel (1018 CS) and 410 Stainless Steel Coupons (410 SS) (Sulfur Content = 1 wt%, AET = 300°C) (a) 410 SS at 2 h; (b) 1018 CS at 2 h ; (c) 410 SS at 4 h, (d) 1018 CS at 4 h; (e) 410 SS at 48 h; (f) 1018 CS at 48 h

Table 4.2 EDX Analyses of the 410 Stainless Steel Coupons Showing Elemental Contents (wt%) of the Areas Indentified in Figure 4.2 (e)

Spectrum	C	Si	S	Mn	Cr	Fe	Total
A	15.7	nil	1.1	0.2	30.8	52.2	100
B	24.3	0.1	4.2	nil	0.4	71.1	100

4.3.2 Influence of sulfur content on corrosion

To study the influence of sulfur content, four oil samples were prepared by adding different quantities of octyl sulfide in white oil with commercial naphthenic acid. The TAN values were 5 mg KOH/g and the sulfur contents were 0.0 wt%, 0.5 wt%, 1.0 wt% and 2.0 wt%. The corrosion rates of carbon steel coupons are plotted in Figure 4.3.

In the liquid phase, the corrosion rates decrease as sulfur content was increased, particularly when the sulfur content was increased from 0.0 wt% to 1.0 wt%. In the vapor phase, the effect of sulfur content was more complicated. When sulfur content was increased from 0.0 wt% to 0.5 wt%, the corrosion rate increased. However as the sulfur contents were increased from 0.5 wt% to 2.0 wt%, the corrosion rates decreased.

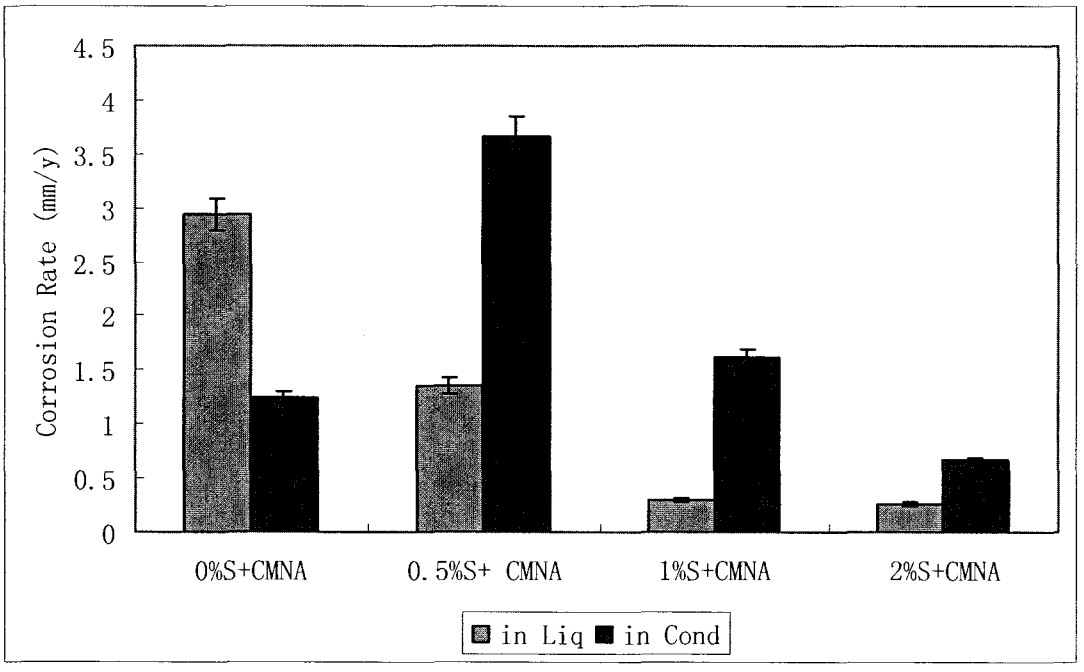

Figure 4.3 Influence of Sulfur Content on Corrosion Rates of Carbon Steel Coupons (TAN = 5 mg KOH/mg, AET = 300°C, Duration = 4h)

4.3.3 Influence of different sulfur compounds on corrosion

The results of the thermal cracking study of sulfur compounds in Chapter 3 demonstrated that different sulfur compounds released hydrogen sulfide at different rates. Consequently, it is expected that not only the contents of the sulfur compounds, but also the types of sulfur compounds play an important role on organic acid corrosion.

In Figure 4.4, organic acid corrosion was much higher when the oil mixture contained diphenyl sulfide than when the oil mixture contained octyl sulfide, even though the sulfur contents were the same for both tests (1 wt%). This was mainly because the octyl sulfide was much less stable than diphenyl sulfide, and so produced much more H_2S at this temperature. Figure 4.4 shows that the presence of octyl sulfide caused a reduction of corrosion rate in the liquid phase, but had little effect on the corrosion rate in vapor phase. The diphenyl sulfide had no effect on the corrosion rate in the liquid phase but actually increased the corrosion rate in vapor phase.

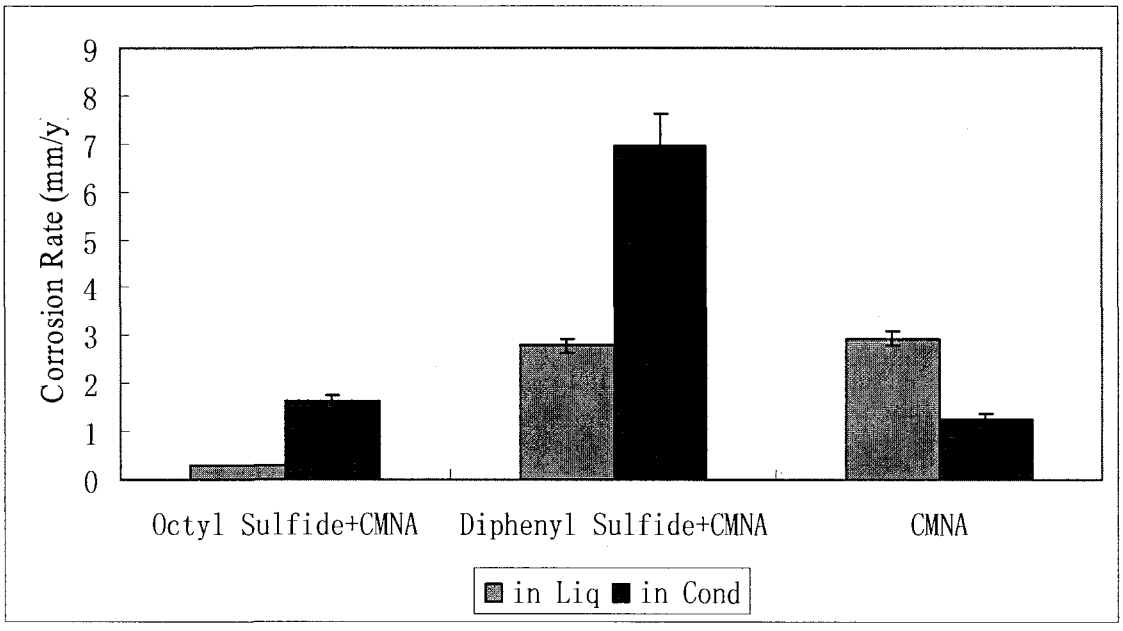

Figure 4.4 Influence of Different Sulfur Compounds (Sulfur Content = 1 wt%) on Corrosion Rates of Carbon Steel Coupons for Commercial Naphthenic Acid (CMNA) in White Oil (TAN = 5 mg KOH/mg, AET = 300°C, Duration = 4h)

Figure 4.5 shows electron micrographs of the carbon steel coupon after the corrosion test with octyl sulfide (1.0 wt%) model oil mixture. The pictures show the cross-sectional morphology at two magnifications. The corresponding EDX spectra for the areas identified in Figure 4.5 (b) are shown below the micrographs in Figure 4.5 (c) to (e).

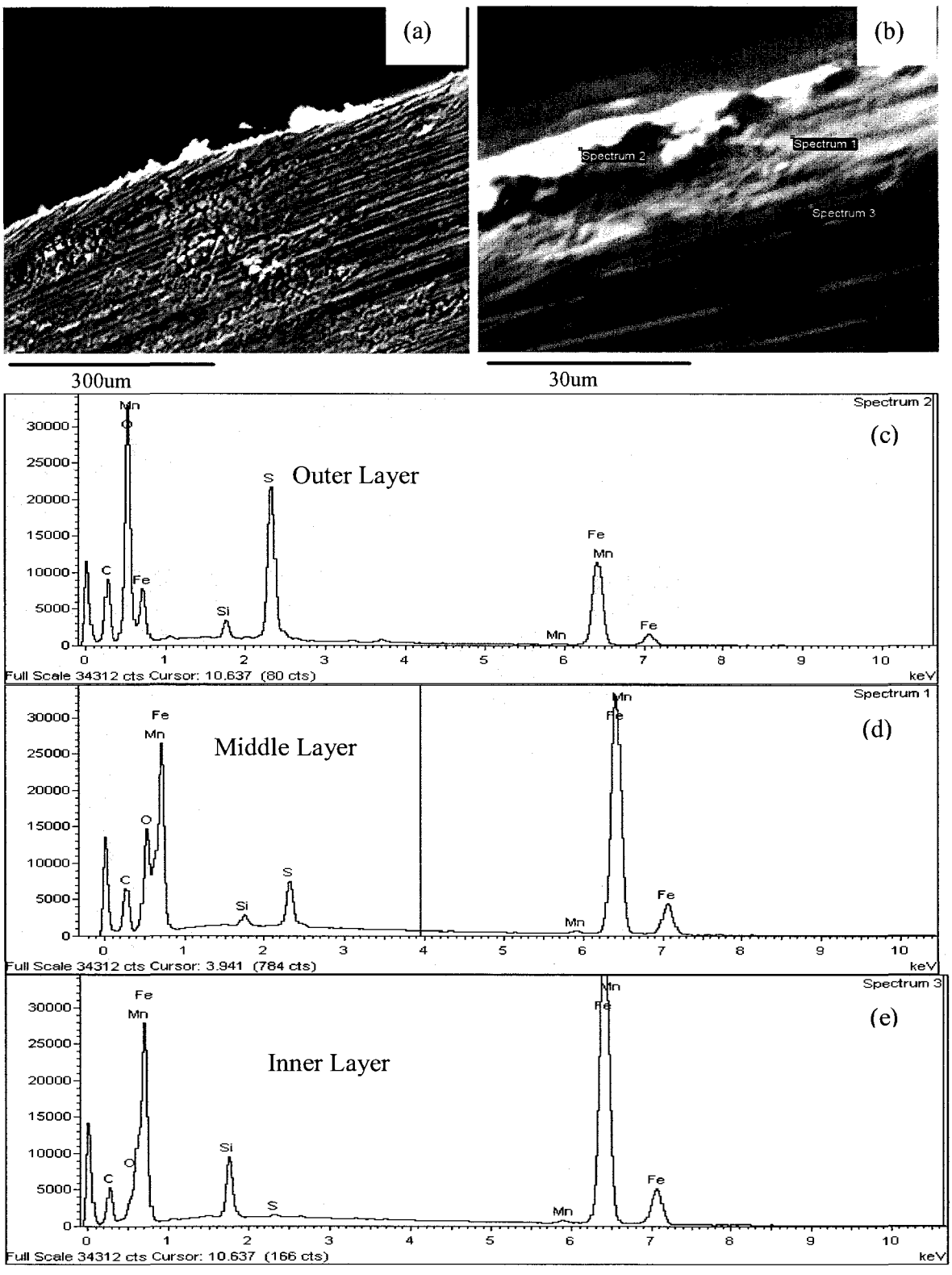

Figure 4.5 SEM and EDX Analyses of Carbon Steel (1wt% Sulfur, TAN = 5 mg KOH/g) (a) Electron Micrograph (Cross-Sectional), (b) 10 Times Magnification of (a), EDX Analyses of Coupon Film (c)Outer Layer, (d) Middle Layer, (e) Inner Layer

Figure 4.5 (a) and (b) show that, the thickness of the film was not even over the surface of the carbon steel coupon, varying from 5 um to 20 um. The film on the carbon steel coupon could be divided into three layers: the outer layer was composed of mainly sulfides and oxides [Figure 4.5 (c)], and the inner layer mainly consisted of metals, such as Fe and Mn with a minor component of sulfur [Figure 4.5 (e)]. The composition of the middle layer was between the two other layers [Figure 4.5 (d)].

4.3.4 influence of different materials on corrosion

Figure 4.6 shows that different materials have different resistances to corrosion. Corrosion rates of both 410 and 316 stainless steels were lower than those of carbon steel under the same experimental conditions, particularly for the corrosion in vapour phase. These results illustrate that the addition of the elements Cr and Mo increase resistance to corrosion. Under the current conditions, the corrosion resistance decreased in the order 316 stainless steel, 410 stainless steel, and carbon steel.

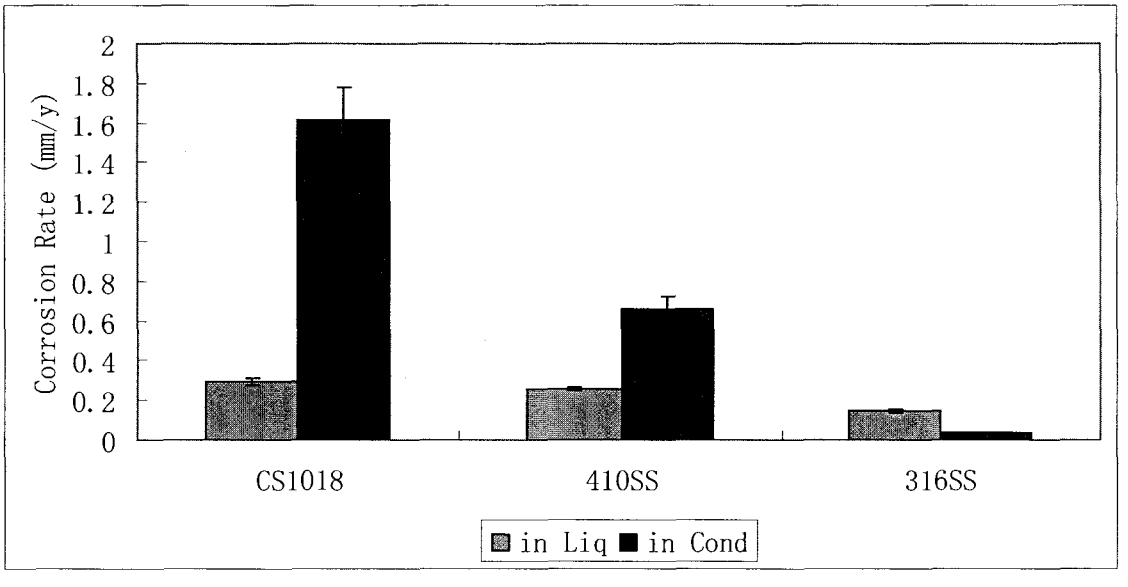

Figure 4.6 Influence of Different Materials on Corrosion Rates for Model Oil Mixtures Containing Commercial Naphthenic Acid and Octyl Sulfide in White Oil (1.0 wt% Sulfur, TAN = 5 mg KOH/g, AET = 300°C, Duration = 4h)

4.4 Discussion

4.4.1 Correlation between corrosivity and sulfur content

As mentioned at beginning of this Chapter, high temperature corrosion is caused by organic acid and hydrogen sulfide attack according to the following equations [22,23]:

$$Fe + 2RCOOH \rightarrow Fe(RCOO)_2 + H_2 \qquad (1.1)$$

$$Fe + H_2S \rightarrow FeS + H_2 \qquad (1.2)$$

$$Fe(RCOO)_2 + H_2S \rightarrow FeS + 2RCOOH \qquad (1.3)$$

Equation (1.1) represents the direct attack of organic acid on iron (carbon steel) where as Equation (1.2) represents the corrosion by hydrogen sulfide. A significant difference between these equations is that, the corrosion product, iron naphthenate, is very soluble in oil, where as iron sulfide is insoluble and therefore tends to precipitate and form a protective film on the metal. It is generally accepted that the forming of metal sulfide films could partly protect the metal from further attack from organic acids and sulfides [9,10,23,34] Equation (1.3) represents the case where hydrogen sulfide reacts with the iron naphthenate to produce iron sulfide. Note that organic acid is regenerated by this reaction. The competition between Equations (1.2) and (1.3) can cause H_2S to inhibit, assist or have no effect on corrosion rates depending on H_2S concentration and process conditions.

These mechanisms help to explain the corrosion test results. For the model oils with 0.0 wt% sulfur content, the corrosion was due to the organic acid attack [Equation (1.1)]. For the model oils with sulfur content, sulfidic corrosion [Equation (1.2)] was introduced and the insoluble corrosion product was deposited on the metal surfaces of coupons. These sulfidic layers (Figure 4.5) acted as barriers for the diffusion of corrosive agents (organic acids and H_2S) through the films, and consequently further corrosion at the metal-film interface was reduced.

For octyl sulfide, as the sulfur content was increased, the quantities of H_2S from

cracking increased resulting in the formation of protective films and the decrease of corrosion rates in liquid phase, as shown in Figure 4.3. For the vapor phase, the same trend was found for sulfur contents between 0.5 wt% and 2 wt%. For sulfur contents between 0.0 wt% and 0.5 wt%, the vapor phase corrosion rate increased (Figure 4.3). This suggests that when sulfur contents were less than 0.5 wt%, the quantity of H_2S generated was too low to produce effective protective film and therefore allowed Equation (1.3) to become the dominant mechanism, causing the corrosion rate to increase.

Some research has found that crude oils need to have 2–3 wt% sulfur content to form the protective layer, as long as the film was not removed [23]. Therefore, a crude oil with relatively high organic acid content and low sulfur content was found to be more corrosive at high temperature than a crude oil with the same organic acid content and high sulfur content [24]. However, the reported total sulfur in crude oil is not a true indication of how corrosive a crude oil will be. The determination of crude oil corrosivity is dependent on the thermal decomposition rates of the different sulfur species to form H_2S.

The results from Chapter 3 showed that sulfur compounds have different cracking behaviors due to their different structures, which means that different sulfur compounds generate different quantities of H_2S at any particular temperature and residence time. So sulfur compounds can be categorized into three types under different thermal conditions. Type I compounds are non-active sulfur compounds, such as dibenzothiophene at 300°C for 2h (Figure 3.9) and diphenyl sulfide at 200°C for 16h (Figure 3.3). Negligible H_2S was produced consequently pure organic acid corrosion would occur under these conditions. Type II compounds are active sulfur compounds, such as octyl sulfide at temperatures above 200 °C (Figure 3.3). More than 50% of the sulfur converted into H_2S and so higher levels of H_2S loading would result in a stable protective film (Figure 4.2). The presence of the film inhibited further corrosion from both organic acids and H_2S (Figure 4.3). Type III compounds are those sulfur species between Type I and Type II, such as diphenyl sulfide at 300°C for 4h. Low levels of H_2S loading in the system assisted corrosion (Figure 4.4). For these types of compounds the quantity of H_2S was too low to form an effective protective film,

similar to the results for octyl sulfide between 0.0 wt% and 0.5 wt% sulfur content. As well, under these conditions Equation (1.3) dominated and organic acids were regenerated.

From the above discussion, it can be concluded that the key factor to determine the influence of sulfur species on corrosion is the quantity of H_2S generated by thermal cracking during the corrosion process. Different quantities of H_2S can inhibit, assist or have no effect on corrosion rates. It would be more accurate to use a measure of "H_2S-generating ability" of crude oil instead of the total sulfur content during corrosivity assessment.

4.4.2 Performance of different materials

Normal construction materials used in crude distillation units are often ranked according to their organic acid corrosion resistance from low to high as carbon steel, 5Cr1/2Mo and 9Cr1Mo low alloy steels, 410, 304, 316 and 317 stainless steels [26,27]. Based on operating experience, 316 and 317 stainless steels have been found to be more resistant to this type of corrosion than carbon steel [15-21].

For the stainless steels, good resistance to organic acid corrosion is attributed to high concentrations of corrosion-resistant elements such as Cr and Mo in the materials [25-31]. Cr is the primary element used to improve corrosion resistance of steels where Cr is believed to promote the oxidation of the metal surface. This oxidation film protects the surfaces of the stainless steels. Consequently addition of Cr increases the resistance of the metal to sulfidic corrosion (Figure 4.2).

Mo has been proven to be the most effective element to resist organic acid corrosion in refineries [30, 32]. With increased Mo content in the stainless steels, both the micro-hardness and the volume fraction of the ferrite are increased. Moreover, Mo has been proven to be beneficial for improving the pitting resistance of stainless steels by promoting film formation on the metal surfaces [21,33]. The preliminary results presented in this work showed the 316 stainless steel with higher Mo content was the most resistant to corrosion. However ever more work is needed to confirm the mechanism involved.

4.5 Summary

A corrosion unit was used to study the influence of sulfur compounds on organic acid corrosion. The oil mixtures were prepared by adding different sulfur compounds and varying the sulfur content in white oil, with or without addition of commercial naphthenic acid.

Sulfidic corrosion depends on H_2S content. Both metal materials and the type of the sulfur compound affects the sulfidic corrosion rate. In the absence of organic acids, octyl sulfide was more corrosive than diphenyl sulfide, as it produced more H_2S at 300°C. 410 stainless steel was more resistant than carbon steel to pure sulfidic corrosion.

Both sulfur content and type play important roles on corrosion rates due to the ability to form H_2S. Octyl sulfide (sulfur content of 1 wt%) produced sufficient protective film to reduce organic acid corrosion at 300°C for carbon steel by an oil mixture containing commercial naphthenic acid (TAN = 5mg KOH/g). The results showed that depending on quantities of H_2S generated, corrosion can be inhibited, assisted or unaffected by the H_2S. Having a measure of the "H_2S-generating ability" of crude oil is more important than the total sulfur content for corrosivity assessment.

Different materials have different resistance to organic acid corrosion in the presence of H_2S. 316 and 410 stainless steels were more resistant than carbon steel. Upon comparison of different materials to organic acid and sulfidic corrosion, it was found that corrosion resistance decreased in order of 316 stainless steel, 410 stainless steel and carbon steel.

4.6 References

[1] A. Jayaraman and R.C. Saxena, Corros. Prev. Control, Vol. 42, No. 6, p. 123, (1995)

[2] Z.A. Foroulis, Anti-corrosion, Vol. 32, No. 11, p. 4, (1985)

[3] A.S. Couper, Corrosion, Vol. 19, No. 11, p. 396, (1963)

[4] A.S. Couper and A. Dravnieks, Corrosion Vol. 18, No. 8, p. 291, (1962).

[5] A.S. Coupper and J.W. Gorman, Mater. Protect. Perform., Vol. 10 No. 1, p. 31, (1971)

[6] K.C. Baker, Mater. Perform. Vol. 40, No. 5, p. 62, (2001)

[7] R.D. Kane and M.S. Cayard, Hydrocarb. Process., Vol. 77, No. 10, p. 97, (1998)

[8] N.R. Smart, A.P. Rance, A.M. Pritchard, Corrosion 2002, NACE Paper No. 02484, (2002)

[9] R.D. Kane, M.S. Cayard, Corrosion 2002, NACE Paper No. 02555, (2002)

[10] "Canada 's Energy Markets: Sources, Transformation and Infrastructure", Natural Resources Canada, <www2.nrcan.gc.ca/es/ener2000/online/html/chap3f_e.cfm> (June 14, 2006).

[11] M.J. Nugent, J.D. Dobis, Corrosion 1998, NACE Paper No. 577, (1998)

[12] M. Paljevic and M. Tudja, Corros. Sci., Vol. 46, No. 8, p. 2055, (2004)

[13] E. Babaian-Kibala, H.L. Craig, G.L. Rusk. Rusk. K.V. Blanchard. T.J. Rose. B.L. Uehlein. R.C. Quinter. M.A. Summers, New Orleans, LA, USA Vol. 93 Paper 631, p. 50, (1993)

[14] K.R. Lewis, M.L. Daane, Corrosion 1999, NACE Paper No. 377, (1999)

[15] D. Johnson, G. McAteer and H. Zuk, Corrosion 2003, NACE Paper No. 03645, (2003)

[16] K. Sugimoto, Y. Sawada, Corros. Sci., Vol. 17, p. 425, (1971)

[17] K. Sugimoto, Y. Sawada, Corrosion, Vol. 32, p. 347, (1976)

[18] H.A. Eldahan, J. Mater. Sci., Vol. 34, p. 851, (1999)

[19] H.A. Eldahan, J. Mater. Sci. Vol. 34, p. 859, (1999)

[20] K. Asami, M. Naka, K. Hashimoto, T. Masumoto, J. Electrochem. Soc., Vol. 127 2130, (1980)

[21] R. Sriram, D. Tromans, Corrosion, Vol. 45, p. 804, (1989)

[22] M.J. Nugent, J.D. Dobis, Corrosion 1998, NACE Paper No. 577, (1998)

[23] M. Paljevic and M. Tudja, Corros. Sci., Vol.46, No. 8, p. 2055, (2004)

[24] E. Babaiankibala, H. Craig Jr., G.L. Lee, K. Rusk, V. Blanchard, T.J. Rose, B.L. Uehlein, R.C. Quinter and M.A. Summers, Mat. Perform, Vol. 32, p. 50, (1993)

[25] S. Tebbal, R.D. Kane, K. Yamada, Corrosion 1997, NACE Paper No. 498, (1997)

[26] K. Sugimoto, Y. Sawada, Corros. Sci., Vol. 17, p. 425, (1971)

[27] K. Sugimoto, Y. Sawada, Corrosion, Vol. 32, p. 347, (1976)

[28] H.A. Eldahan, J. Mater. Sci., Vol. 34, p. 851, (1999)

[29] H.A. Eldahan, J. Mater. Sci. Vol. 34, p. 859, (1999)

[30] K. Asami, M. Naka, K. Hashimoto, T. Masumoto, J. Electrochem. Soc., Vol. 127, p. 2130, (1980)

[31] R. Sriram and D. Tromans. Corrosion, Vol. 45, p. 804, (1989)

[32] H. Lee Craig, Jr., Corrosion 1996, NACE Paper No. 603, (1996)

[33] H.A. Eldahan, J. Mater. Sci. Vol. 34, p. 851, (1999)

[34] X.Q. Wu, H.M. Jing, Y.G. Zheng, Z.M. Yao and W. Ke, Corrosion Science, Vol. 46, No. 4, p. 1013, (2004)

Chapter 5. Investigation of Athabasca Bitumen Corrosivity

5.1 Introduction

In this work it was found that molecular weights, structures, and boiling points of organic acids influence their high temperature corrosivity. These acids are distributed differently in different crude oils and petroleum fractions. Consequently, this is at least part of the explanation for why there is poor correlation between TAN and corrosivity of crude oils [1-7]. Another part of the explanation would be due to sulfur species. Sulfur compounds occur in crude oils at various concentrations, and consist of various types of chemical structures. Consequently sulfur conversion to hydrogen sulfide is different for different sulfur compounds over the temperature range of 220-400°C [8-12]. As discussed in Chapter 4, the presence of hydrogen sulfide can enhance, inhibit or have no effect on organic acid corrosion.

To be able to relate the corrosion results from the model oils consisting of specific organic acids and sulfur compounds in white oil to those for crude oils, the following approach was taken. First, the organic acids from a crude oil were isolated and characterized using high temperature simulated distillation, and elemental and nuclear magnetic resonance (NMR) carbon-type analyses. The commercial naphthenic acid used throughout this thesis was characterized similarly. Next, model oil mixtures were prepared with either the organic acids isolated from Athabasca bitumen or the commercial naphthenic acid. Finally, the corrosivity of the model oil mixtures and Athabasca bitumen were measured and compared.

5.2 Experimental Procedures

5.2.1 Materials and media

The Athabasca bitumen sample was produced by steam assisted gravity

drainage at the Underground Test Facility close to Fort McMurray, Alberta. The organic acids from Athabasca bitumen were isolated using the ion-exchange separation method for selective isolation of carboxylic acids from crude oils [13]. The white oil (Klearol, boiling point [b.p.] 227-512°C) and the commercial naphthenic acid mixture were the same as mentioned in earlier chapters, and carbon steel coupons were used for corrosion testing.

The model mixture containing the organic acids isolated from Athabasca bitumen was reconstituted to the same TAN as the original bitumen, 3.4 mg KOH/g. The commercial naphthenic acid in white oil were prepared to a TAN of 5.0 mg KOH/g. The TAN values were confirmed using the CCQTA-modified ASTM D664 method in units of mg KOH/g of oil.

5.2.2 Corrosion test method

The corrosion apparatus and operating procedures were the same as those described in Chapter 2 and Chapter 4. The temperature of 250°C and vacuum of 300 mbar were used to achieve the equivalent temperature (AET) of 300°C. Metal coupon specimens were degreased by washing in acetone, dried in air and weighed before tests. After tests, specimens were carefully rinsed with acetone to maintain films, dried in air and observed by electron microscopy to study morphology. Finally, corrosion films were washed in acetone, and specimens were rinsed under running water, rinsed in distilled water, and then dried in air and weighed. The corrosion rate was calculated in the same way as in Chapter 3.

5.2.3 Analytical methods

High-temperature simulated distillation was performed on an Agilent gas chromatograph using Analytical Control software (American Society for Testing and Materials [ASTM] 6352-02).

Elemental analyses were run at the University of Alberta Chemical Services. The contents of carbon, hydrogen, nitrogen, sulphur and oxygen were run on the same instrument, a Carlo Erba EA-1108 CHNS-O Elemental Analyzer, following instrument procedure.

^{1}H NMR samples were prepared by mixing approximately 20 mg of the sample with 700 μL deuterochloroform ($CDCl_3$). For ^{13}C NMR spectra, approximately 50 mg of the sample was dissolved in 700 μL $CDCl_3$. The NMR experiments were performed at room temperature (20 ± 1 °C) on a Varian Unity 600 NMR spectrometer, operating at 599.735 MHz for proton and 150.818 MHz for carbon. Carbon type analyses were performed using proton and carbon NMR spectra, and elemental analysis results using a procedure based on that described by Japanwala *et. al.* [14].

Carbonyl carbon contents of samples were measured using Fourier transform infrared spectroscopy. Spectra were collected on a Bruker FT-IR spectrometer (model Tensor 27). Samples were prepared to 50 mg/mL in methylene chloride and analyzed in a solution potassium bromide cell (0.5 mm path length). Quantification of carbonyl contents were performed by use of a standard curve prepared using known quantities of model compounds in methylene chloride. Peak areas in the region of 1650 cm^{-1} to 1800 cm^{-1} were used.

A HITACHI S-2500 scanning electron microscope with INCAx-act energy dispersive x-ray spectroscopy (EDX) capability was used for morphology observation and composition analyses of coupon surfaces. Measurements were performed at room temperature using a 20 kV accelerating voltage.

5.3 Results and Discussion

Figure 5.1 shows corrosion rates of carbon steel coupons for model oil mixtures prepared in white oil using commercial naphthenic acid or organic acids isolated from Athabasca bitumen (ATHBA), and Athabasca bitumen (ATHB). Coupons were located either in liquid, or in vapor phase where the acids condensed on the coupon surfaces (condensate). Figure 2.3 showed that there is a linear relationship between corrosion rates and TAN values under the corrosion test conditions chosen. This relationship was

used to adjust the corrosion rates for ATHBA model oil and ATHB to a TAN of 5.0 mg KOH/g[2]. The high temperature simulated distillation results for the commercial naphthenic acid and ATHBA are shown in Figure 5.2.

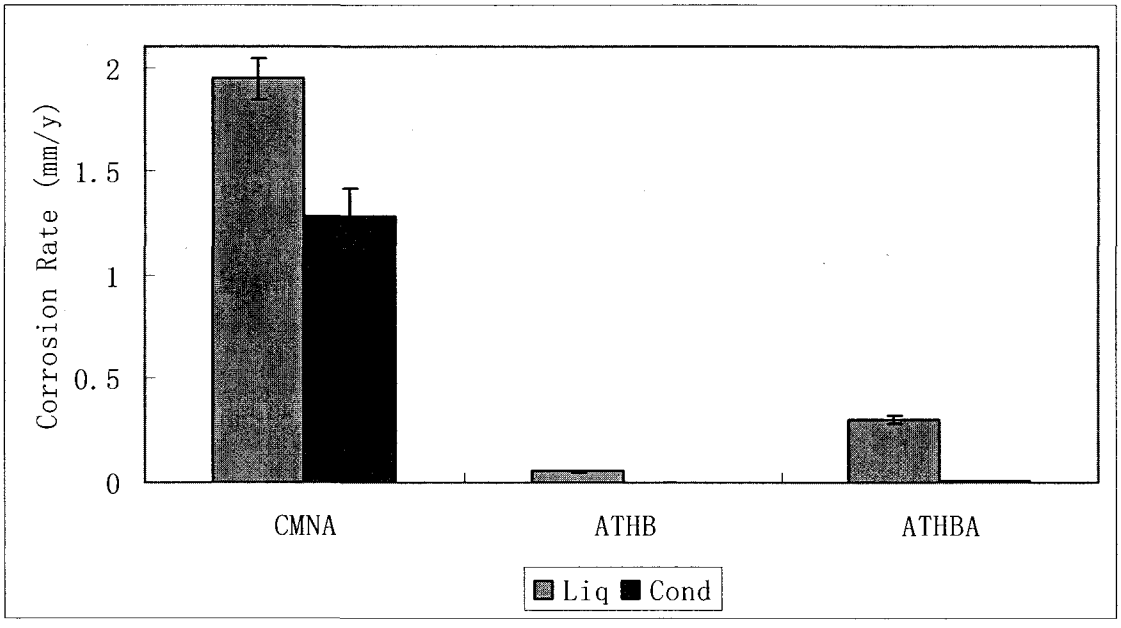

Figure 5.1 Corrosion Rates of Carbon Steel Coupons for Commercial Naphthenic Acid (CMNA) and ATHBA in White Oil, and ATHB in Liquid (Liq) and Condensate (Cond) (AET = 300°C, TAN = 5 mg KOH/g)

[2] The commercial naphthenic acid is more corrosive than the ATHB and ATHBA so use of this correlation will slightly over-estimate the ATHB and ATHBA corrosion rates at TAN values of 5.0 mg KOH/g

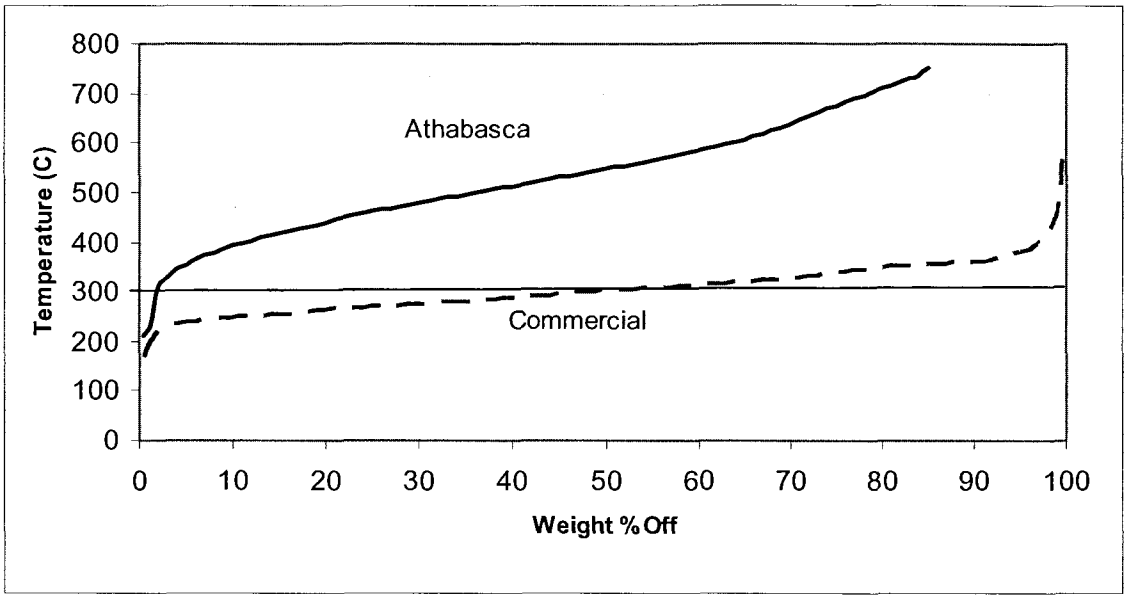

Figure 5.2 High Temperature Simulated Distillation Results for the Commercial Naphthenic Acid and the ATHBA

5.3.1 Influence of organic acid composition on corrosivity

Figure 5.1 shows that the commercial naphthenic acid is much more corrosive than ATHB both in liquid and condensate. The corrosivity differences of the carbon steel coupons in condensate can easily be explained by referring to the high temperature simulated distillation plots in Figure 5.2. At the AET of 300°C chosen, 50 wt% of the commercial naphthenic acid and less than 2 wt% of the Athabasca organic acids were above their boiling points. As found with the specific organic acids compounds in Chapter 2, corrosion in condensate can only occur when the AET is above their boiling point. Over 98 wt% of the Athabasca organic acids remain in the oil liquid and only 2 wt% of the Athabasca organic acids would contribute to the corrosion in condensate. This explains the negligible corrosion rate for ATHB in condensate

On comparing the corrosion of carbon steel coupons immersed in the oil liquids, the corrosion rate of the commercial naphthenic acid is significantly higher than that of the Athabasca samples even after adjusting to the same TAN value. Some explanation

is offered from the high temperature simulated distillation results as the smallest boiling acid molecules were found to be the most corrosive in the liquid (Figure 2.7). Further insight comes from comparison of the carbon type compositions obtained from elemental, nuclear magnetic resonance, and Fourier transform infrared analyses shown in Table 5.1.

Table 5.1 NMR Carbon Type Analyses

Carbon Type	Carbon Content (mole%)	
	Commercial Naphthenic Acid	ATHBA
Aromatic	5.7	26.9
Cycloparaffinic	41.0	28.1
Branched Paraffin	8.2	7.1
Paraffin Chain (C1+)	37.6	34.8
Olefin	0.4	0.1
Carboxyl Group	7.1	3.0
Total	100.0	100.0

The greatest differences in composition between the commercial naphthenic acid and the ATHBA are the aromatic and cycloparaffinic carbon contents. The contents of aromatic and cycloparaffinic carbon in ATHBA are similar and account for approximately half of the carbon. In contrast, the commercial naphthenic acid has a low content of aromatic carbon and almost half of its carbon is cycloparaffinic. The small olefinic carbon content in ATHBA does not result from the presence of cracked product as history of the sample is known. The double bonds likely are part of porphorynic structures associated with the asphaltenes in the acids [15]

Carbon type analyses also allow average structural features such as ring cluster size and chain segment length to be calculated. The results are shown in Table 5.2. The small content of aromatic carbon is associated with 1-ring (6 carbon) aromatic species. In ATHBA, on average aromatic species are between 2 rings (10 carbons) and 3 rings (14 carbons) in size. The cycloparaffinic ring clusters and average chain segment lengths are similar. Figure 5.3 illustrates the structural features suggested by the carbon type analyses results. From ^{13}C NMR spectroscopy, the acid groups in commercial naphthenic acid are attached to both cycloparaffin rings and chain ends where as in

ATHBA, most of the acid groups are attached to the ends of chains (data not shown).

Table 5.2 Additional Information from Carbon Type Analyses

Structural Feature	Commercial Naphthenic Acid	ATHBA
Aromatic carbon cluster size	6 (1 ring)	11 (2-3 rings)
Cycloparaffinic carbon cluster size	9 (1-2 rings)	8 (1-2 rings)
Average chain-segment length	2.0	3.1

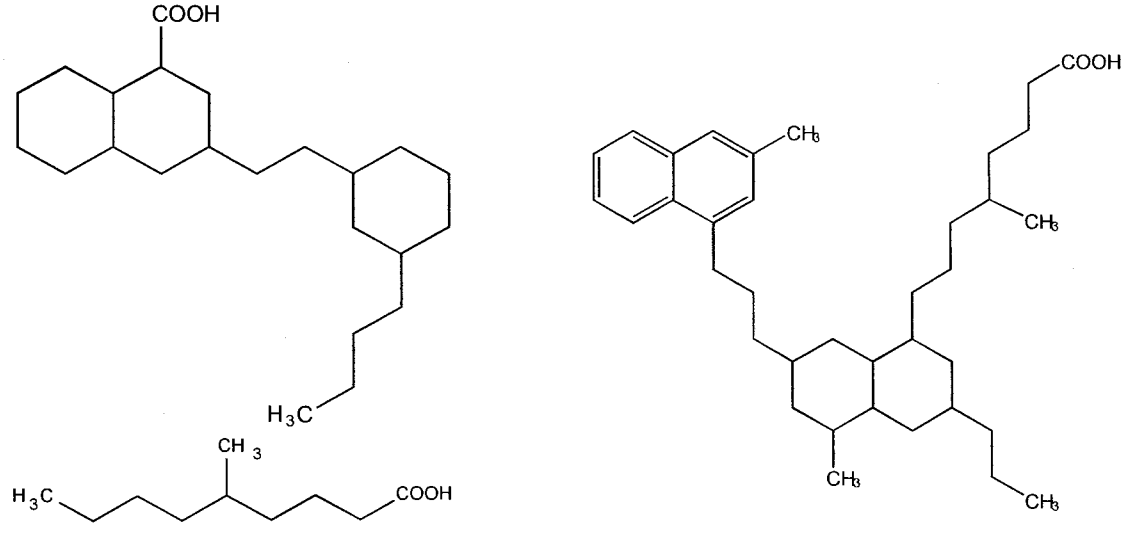

CMNA **ATHBA**

Figure 5.3 Representative Structures for the Commercial Naphthenic Acid (CMNA) and ATHBA

As illustrated in Figure 5.3, not only does the commercial naphthenic acid consist of smaller species (shown by high temperature simulated distillation), but it has lower ring content. In Chapter 2, it was concluded that the organic acids with the lowest molecular weights and ring content were the most corrosive. For the organic acid mixtures found in crude oils, these results can be also applied using NMR and high temperature simulated distillation results. Of the two model oil mixtures, the commercial naphthenic acid was characterized as having relatively lower average

carbon numbers and smaller ring cluster size than those of ATHBA. Consequently it is expected that the corrosion rates for the commercial naphthenic acid was higher than that for ATHBA.

Figure 5.1 shows a second interesting result. For the same TAN value and organic acid composition, ATHBA was more corrosive than the original bitumen. This suggests that there is (at least) one more factor influencing corrosivity other than the organic acids (discussed below).

5.3.2 Influence of sulfur species on organic acid corrosion for Athabasca bitumen

For the same TAN value and organic acid composition, the isolated organic acids from Athabasca bitumen dissolved in white oil were more corrosive than the original bitumen (Figure 5.1). This suggests that there is (at least) one more factor influencing corrosivity other than the organic acids.

A significant difference between the coupons exposed to ATHB and those exposed to ATHBA was that a black corrosion film product appeared on the ATHB coupon, detectible by naked eye. Figure 5.4 shows the scanning electron micrographs of the coupons after the corrosion tests for ATHB [Figure 5.4 (a)] and ATHBA. [Figure 5.4 (b)] Figure 5.4 (a) shows that a layer of film can be observed on the surface of the coupon after the corrosion test with ATHB. In Figure 5.5, the composition analyses of the metal surfaces were performed using EDX. The results shown in Figure 5.5 (a) indicate that area A in Figure 5.4 has a high content of metal sulfides. This film appears to have given some protection for the metal surface from corrosion attack. Figure 5.4 (b) shows the surface of the carbon steel coupon after the corrosion test for the ATHBA where black spots are visible i.e. area B in Figure 5.4 (b). In this case, metal sulfides can also be detected but are in low concentration [Figure 5.5 (b)]. As well, the extent of the coverage was too low to form an effective protective film over the fresh metal.

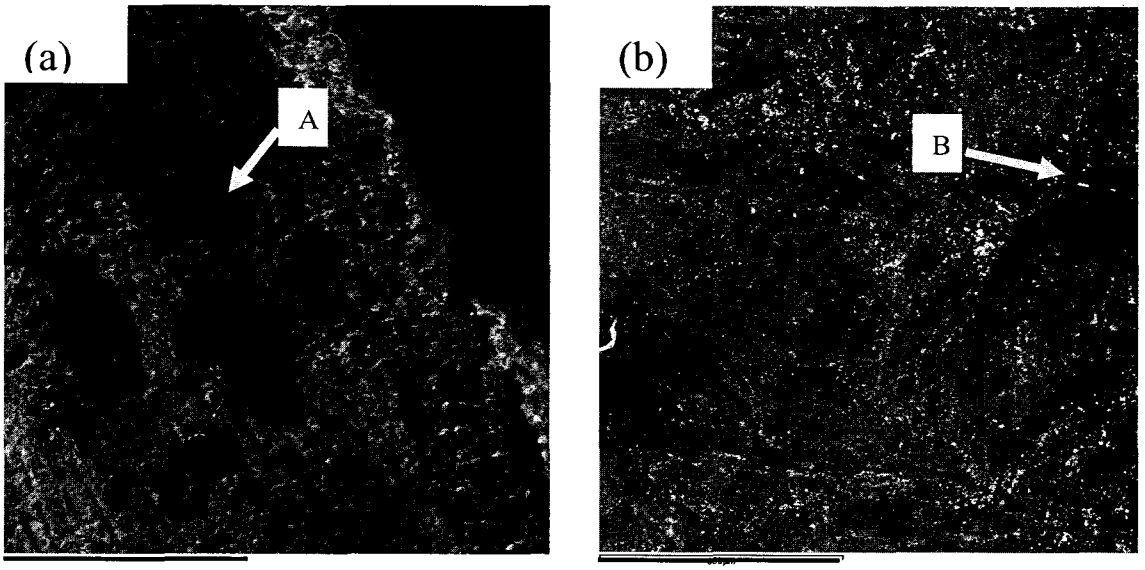

Figure 5.4 Electron Micrographs of Carbon Steel Coupons after Corrosion with (a) ATHB and (b) ATHBA

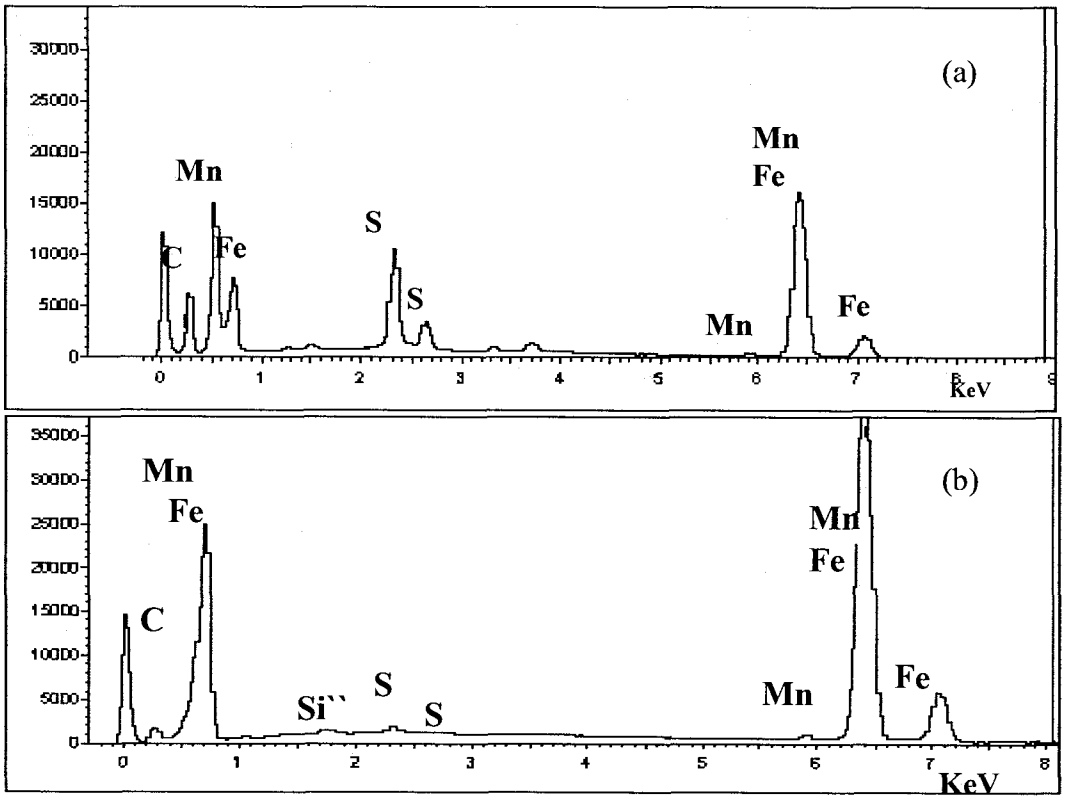

Figure 5.5 EDX Analyses of Carbon Steel Coupons Showing Figure 5.4 (a) Area A and (b) Area B

These results show that the ATHB has a greater content of sulfur than ATHBA. This is certainly the case as the sulfur content of the white oil medium was negligible where as Athabasca bitumen had sulfur content of 4.8 wt% from the elemental analyses as shown in Table 5.3.

Table 5.3 Elemental Analyses of ATHB, ATHBA and Commercial Naphthenic Acid

Element:	Content (wt%)		
	ATHB	ATHBA	Commercial Naphthenic Acid
Carbon	84.7	79.4	74.4
Hydrogen	10.1	10.5	12.0
Nitrogen	0.4	0.4	0.00
Sulphur	4.8	3.8	0.00
Oxygen	-*	5.9	13.7

* Not measured

5.4 Summary

In the present study, a laboratory-scale corrosion unit using carbon steel coupons has been used to study how the composition of organic acid and sulfur species of Athabasca bitumen influences its corrosivity. Measurements were obtained from coupons located both in the liquid, and in the vapor phase where the acids condense on the surface. Corrosion measurements were run for model oil mixtures using either commercial naphthenic acids or organic acids isolated from Athabasca bitumen for comparison with that of the original Athabasca bitumen.

When the corrosion rates of the commercial naphthenic acid in white oil was compared to those of the organic acids isolated from Athabasca bitumen in white oil, the results showed that organic acids from Athabasca bitumen were much less corrosive. The low corrosivity is mainly due to the composition of the organic acids from Athabasca bitumen which consist of higher boiling acid species with higher ring contents. Interestingly, the original Athabasca bitumen was less corrosive than its isolated organic acids reconstituted in white oil. Inspection of the coupons by scanning

electron microscopy indicated that iron sulfide deposition during the Athabasca bitumen corrosion test partially protected the metal surface. These results illustrate the same behaviors found for the model oil mixtures described in Chapters 2 and 4.

5.5 References

[1] R.L. Piehl, Corrosion, 1987, NACE Paper No. 196, (1987)

[2] A. Turnbull, E. Slavcheva and B. Shone, Corrosion, Vol. 54, No. 11, p. 922. (1998)

[3] M.P. Barrow, L.A. McDonnell, X.D. Feng, J. Walker and P.J. Derrick, Anal. Chem. Vol.75, No. 4, p. 860, (2003)

[4] S. Tebbal and R. Kane, Corrosion 1998, NACE Paper No. 578, (1998)

[5] G.C. Laredo, C.R. Lopez, R.E. Alvarez and J.L. Cano, Fuel, Vol. 83, No.11, p. 1689, (2004)

[6] B. Messer, B. Tarleton, M. Beaton, T. Phillips, Corrosion 2004, NACE Paper No. 04634, (2004)

[7] B.F. Qi, X. Fei, S.J. Wang and L.R. Chen, Pet. Sci. Technol. Vol. 22, No.3–4, p. 463, (2004)

[8] A. Jayaraman and R.C. Saxena, Corros. Prev. Control, Vol. 42, No. 6, p. 123, (1995)

[9] Z.A. Foroulis, Anti-corrosion, Vol. 32, No. 11, p. 4, (1985)

[10] A.S. Couper, Corrosion, Vol. 19, No. 11, p. 396, (1963)

[11] A.S. Couper and A. Dravnieks, Corrosion Vol. 18, No. 8, p. 291, (1962).

[12] A.S. Couper and J.W. Gorman, Mater. Protect. Perform., Vol. 10 No. 1, p. 31, (1971)

[13] H. Mediaas, K.V. Grande, B.M. Hustad, A. Rasch, H.G. Rueslåtten, J.E. Vindstad, Society of Petroleum Engineers, paper 80404, (2003)

[14] S. Japanwala, K.H. Chung, H.D. Dettman, and M.R. Gray, Energy & Fuels, Vol. 16, p. 477, (2002)

[15] S. L. Salmon, D. Zinz, and H.D. Dettman, presented at the "Petroleum Phase Behavior and Fouling Conference", Victoria, Canada, (2008)

Chapter 6. Conclusions and Future Directions

6.1 Conclusions

High temperature corrosion is complex because of the multiple interdependent parameters such as temperature, materials, TAN value, molecular structure, and sulfur content [1-9]. These factors have been studied in this project. Particular emphasis was placed on properties of the organic acids and the interactions of organic acids and sulfur compounds.

A corrosion unit has been developed to simulate corrosion found in refinery vacuum distillation towers where corrosion both in liquid and in vapor phase, where organic acids condense on metal surfaces, exists. For each corrosion test, model oil mixtures were prepared with various TAN values, organic acid types, sulfur compound types and total sulfur contents using organic acids or/and sulfur compounds dissolved in white oil. Corrosion measurements were run for the model oil mixtures and compared with that of virgin Athabasca bitumen.

For the commercial naphthenic acid in white oil, corrosion rates for carbon steel coupons suspended in the vapor phase increased with increasing TAN value and temperature where as the corrosion rates for the coupons immersed in the oil liquid increased with TAN value only. These results were expected as they reflect increases in acid concentration either in vapor phase or in the oil liquid.

When individual organic acid compounds in white oil were tested for corrosivity, several conclusions were made. For corrosion of carbon steel coupons suspended in the vapor phase, the boiling point of the organic acids was a threshold temperature for corrosion. If the atmospheric equivalent temperature (AET) was below the boiling point, there was little corrosion; if the AET was above the boiling point, the lowest molecular weight, straight chain carboxylic acid was the most corrosive. For carbon steel coupons immersed in the oil liquid, the corrosion decreased with

increasing molecular weight of the organic acid. The corrosion rates in the liquid were lower than those obtained in the vapor phase when AET was above the organic acid boiling point and were comparable to those found in the vapor phase when AET was lower than the boiling point.

When the corrosion rates of the commercial naphthenic acid in white oil was compared to those of the organic acids isolated from Athabasca bitumen in white oil, and the original Athabasca bitumen, the following conclusions were made. Because the commercial naphthenic acid consisted of lower boiling acid species with lower ring contents, it was the most corrosive for coupons located both in the vapor phase and in the oil liquid.

The influence of sulfur compounds on organic acid corrosion was related to their ability to decompose into H_2S combined with the resistance of the metal to sulfidic corrosion. All sulfur compounds tested except dibenzothiophene decomposed and produced H_2S not only in gas form but also dissolved in the liquid product. Different sulfides have different H_2S yield under the same conditions. At 300°C and 2 h residence time, benzyl sulfide produced more H_2S gas than the others tested where as dibenzothiophene conversion was negligible.

Sulfur conversion was different for different sulfur compounds at any particular temperature and residence time because of the different chemical bond structures. The thermal stabilities of the C-S bonds in ring structures were greater than those in chains. If the C-S bonds were between two aromatic rings, such as diphenyl sulfide and benzyl phenyl sulfide, the methylene C-S bond in benzyl phenyl sulfide was easiest to break.

Sulfur compounds caused sulfidic corrosion due their thermal decomposition and formation of H_2S. Given the high conversions obtained at 200°C for octyl and dodecyl sulfide, these types of sulfur compounds would begin to thermally decompose at temperatures less than 200°C. Consequently, the H_2S generated from these compounds would contribute to sulfidic corrosion under these conditions. As well, materials affect the sulfidic corrosion rates. For example, 410 stainless steel was more resistant than carbon steel to pure sulfidic corrosion.

Both sulfur content and sulfur compound type can play an important role during organic acid corrosion due to the potential ability to form sulfide films. According to

the corrosion mechanism, the presence of H_2S could inhibit, assist or have no effect on corrosion rates depending on H_2S concentration and process conditions. For example, octyl sulfide in oil mixture at a sulfur content of 1 wt% produced sufficient protective film to reduce organic acid corrosion of carbon steel (AET = 300°C, TAN = 5 mg KOH/g). For octyl sulfide at a sulfur content of 0.5 wt%, corrosion rates in vapor phase were increased under the same conditions. In this case, there was enough H_2S produced to regenerate the organic acids but not enough iron sulfide formed to create a protective film. Consequently, having a measure of the "H_2S-generating ability" of crude oil is more important than the total sulfur content for corrosivity assessment. Because of its sulfur content, the virgin Athabasca bitumen was significantly less corrosive than the organic acids isolated from Athabasca bitumen reconstituted in white oil. This indicated that the black iron sulfide deposit formed during the Athabasca bitumen corrosion test partially protected the metal surface. When carbon steel coupons were replaced with 316 or 410 stainless steel coupons, corrosion rates were decreased. These results demonstrated that the addition of chromium and molybdenum increased the resistance of the materials to corrosion.

6.2 Future Directions

6.2.1 Chemical analyses of the crude oils

In order to find a reliable quantitative correlation between chemical composition of crude oils and their corrosivity, further corrosion studies with more powerful analytical methods for identification of oil constituents are required. Chemical analyses of the crude when correlated to refinery corrosion experience are believed to be the most promising method for predicting the corrosivity of a crude oil. TAN values and sulfur content are readily available in crude assays but provide poor prediction of the corrosivity. In this paper, some of the relationships between the chemical properties, such as the molecular structure of organic acid and sulfur compounds, and their corrosiviities have been studied. Additional chemical analyses such as hydrogen sulfide evolution with temperature of crude oils and organic acid

decomposition with temperature would also be useful in assessing crude corrosivity. Finally greater understanding of the nature of films formed in the alloyed material and the level of H_2S needed to inhibit organic acid corrosion would be necessary to complete the explanation of the results of this study, and to assist in extrapolating this work to service conditions.

6.2.2 Process simulation with fluid velocity.

The corrosion unit used in this study simulates high temperature corrosion in distillation towers of refineries where condensation of vaporized organic acids occurs on the walls and tower trays. Under these conditions, fluid velocity has virtually no effect on the corrosion process. However, high temperature corrosion also occurs in the transfer lines and furnace tubes. In these parts of the refinery, fluid flows play an important role [11]. The contributions of velocity or, more accurately, wall shear stress, needs to be considered. To estimate wall shear stress, it is necessary to know the density and viscosity of the liquid and the vapor, the degree of vaporization and the pipe diameter. Plots of diameter versus roughness, and friction factors (Moody Diagram) are also needed. First, the Reynold's number for field flow conditions in a pipe is calculated by the following equation [12]:

$$R_e = D \rho V / \mu$$

where R_e = Reynold's number

D = diameter of pipe (m)

ρ = density of fluid (Kg/m^3)

V = velocity of fluid (m/s)

μ = dynamic viscosity (Kg/m.s, 1 Poise = 0.1 Kg/m.s)

With the Reynold's number known, the relative roughness (e/D) is obtained from the plot of diameter versus relative roughness, and the friction factor (f) is then obtained from the Moody Diagram. Finally, the shear stress (τ) is calculated by the following equation [13]:

$\tau = f \rho V^2 / 2$

where f is the friction factor

ρ = density of fluid (Kg/m^3)

V = velocity of fluid (m/s)

To use plant corrosion data of a specific crude or blend to predict its corrosivity in another plant, the following approach is taken: (1) calculate shear stress values around the plant with known corrosion data; (2) calculate shear stress for similar locations in a plant which is planning to run the specific crude or blend and (3) compare the values of shear stress. Corrosion rates can be estimated as they are directly proportional to shear stress. Typically, the higher the acid content, the greater is the sensitivity to shear stress. When high temperature and high shear stress are combined, even very low levels of organic acid may result in very high corrosion rates. For future laboratory studies, a new corrosion unit needs to be designed and built to introduce the effects of the shear stress. In this corrosion unit, the model oil mixtures studied above could be tested under different temperature and flow conditions to assess the importance of chemical properties and wall shear stress to corrosivity.

6.2.3 The correlation between laboratory test and crude corrosivity assessment

High temperature corrosion can be complex as the organic acids and sulfur species in crude oils can vary considerably with their source. However, industry surveys indicated that refiners still heavily depend on previous experience in assessing the corrosivity of crude feeds [10, 11]. It is commonly observed that organic acid corrosion behaviors in lab tests are different from high temperature corrosion in refinery environments. One reason for discrepancies between lab and plant results could be that the lab samples do not accurately reflect the reactivity of the refinery crude sample due to differences in content of types of organic acids and sulfur species as discussed in this thesis. Consequently chemical characterization of organic acids from other crude oils, and measurement of their corrosivity, as presented for the commercial naphthenic acid and Athabasca bitumen, will help to assess how accurately

the contributing factors identified in this work extrapolate to crude oil corrosivity.

Secondly, the conclusions of the present study are based on short-term lab experiments. Initial results showed that organic acids corrosivity decreases with run time of the experiment. If the results herein tend to overestimate corrosion rates found in refinery distillation units, then a longer run time may be chosen to better correlate with refinery benchmarks.

Finally, the effect of flow conditions that make significant contributions to corrosion in high temperature refining environments was not considered in this paper. Consequently, it would not be appropriate to extrapolate results from this study to a system that includes flow conditions. However, the present lab results do provide new information towards the understanding of molecular factors affecting organic acid corrosion, sulfidic corrosion, and their influence on each other. This information forms a good base for future corrosion studies.

6.3 References

[1] E. Slavcheva, B. Shone and A. Turnbull, Br. Corrosion. J., Vol. 34, No. 2, p. 125, (1999)

[2] R.D. Kane and M.S. Cayard, Hydrocarb. Process., Vol.74, No11, p. 129, (1995).

[3] W. P. Jepson, Corrosion 1997. NACE Paper No. 11, (1997)

[3] M. V. Enzien, Corrosion 1996, NACE Paper No. 290, (1996)

[4] E. Slavcheva, B. Shone, A. Turnbull, Corrosion 1998, NACE Paper No. 579, (1998)

[5] H. J. D. Bruyn, Corrosion 1998, NACE Paper No. 576, (1998)

[7] G.L. Scattergood, R.C. Strong, W.A. Lindley, Corrosion 1987, NACE Paper No.197, (1987)

[8] B.E. Hopkinson, L.E. Penuela, Corrosion 1997, NACE Paper No. 502, (1997)

[9] H. L. Craig, Corrosion 1995, NACE Paper No. 333, (1995)

[10] D. Johnson, G. McAteer, H. Zuk, Corrosion2003, NACE Paper No. 03645

[11] R.D. Kane, M.S. Cayard, Hydrocarb. Process. Vol. 77, No. 10, p. 97, (1998)

[12] A. Demoz, T. Dabros, K. Michaelian, and W. Revie, Corrosion Vol. 60, p. 455, (2004)

[13] B. Massey and J. Ward-Smith, Mechanics of fluids, seventh ed., Stanley Thorns Pub. Ltd., p. 197, (1998)